EVALUATION OF DAMPING CONTROL OF A UNIFIED POWER FLOW CONTROLLER

BY

MOHAMMED ABDULRAOUF AL-GHAZWI

A Thesis Presented to the
DEANSHIP OF GRADUATE STUDIES

KING FAHD UNIVERSITY OF PETROLEUM & MINERALS

DHAHRAN, SAUDI ARABIA

In Partial Fulfillment of the
Requirements for the Degree of

MASTER OF SCIENCE

In

ELECTRICAL ENGINEERING

JUNE 2009

KING FAHD UNIVERSITY OF PETROLEUM & MINERALS

DHAHRAN 31261, SAUDI ARABIA

DEANSHIP OF GRADUATE STUDIES

This thesis, written by **MOHAMMED ABDULRAOUF AL-GHAZWI** under the direction of this Thesis Advisor and approved by his Thesis Committee, has been presented to and accepted by the Dean of Graduate Studies, in partial fulfillment of the requirements for the degree of **MASTER OF SCIENCE IN ELECTRICAL ENGINEERING.**

Thesis Committee

Dr. Abu Hamed M. Abdur-Rahim (Chairman)

Dr. Ibrahim M. El-Amin (Chairman)

Dr. Ibrahim Habiballah (Member)

Dr. Samir A. Al-Baiyat (Member)

Dr. Mohammad A. Abido (Member)

Dr. Samir H. Abdul-Jauwad
Department Chairman

Dr. Salam A. Zummo
Dean of Graduate Studies

6/7/09
Date

Dedicated
to
My Father, Mother, Wife
and
Brothers, Sisters

I am deeply indebted to my thesis advisor Dr. Abu Hamed Abdur-Rahim for his constant support, guidance, encouragement and constructive criticism through out the course of this research. I will always revere his patience, expert guidance and ability to solve intricate problems. He made my pursuit of higher education a truly enjoyable and unforgettable experience. At the later stages he helped me a lot in writing my thesis. I could not have imagined having a better advisor and mentor for my study.

I am also grateful to my co-advisor, Dr. Ibrahim, El-Amin, for reading previous drafts of this dissertation and providing many valuable comments that improved the presentation and contents of this dissertation.

I would also like to thank my committee members Dr. Samir A. Al-Baiyat, Dr. Ibrahim Habiballah, and Dr. Mohammed. A. Abido for their encouragement, cooperation and for spending their time reading my thesis and for their constructive comments and suggestions.

Lastly but not the least, I would like to give my special thanks to my parents, brothers and sisters especially my wife for their tireless support, encouragement and prayers in all my endeavors. Their knowledge, sacrifice and love, has helped me achieve all my goals to date.

TABLE OF CONTENTS

List of Tables

List of Figures

NOMENCLATURE

Symbols

x	Transmission Line Reactance
H	Inertia Constant
M	Inertia Coefficient, M=2H
D	Damping Coefficient
p.u.	Per Unit Quantities
pf	Power Factor
P_e	Electrical Power Output to the Machine
e_q	Internal Voltage across x_q
V_t	Machine Terminal Voltage
V_e	Sending end Voltage
V_b	Infinite Bus Bar Voltage
V_c	DC-Link Capacitor Voltage
e_e	Magnitude of Voltage E_s, the Input Voltage of Shunt Converter
e_b	Magnitude of Voltage E_b, the Input Voltage of Series Converter
P_m	Mechanical Power Output to the Machine
$e_q^{'}$	Internal Voltage on q-Axis Proportional to Field Flux Linkage
E_{fd}	Generator Field Voltage

$T_{do}^{'}$	Direct Axis Open-Circuit Field Time Constant
K_r	Exciter Gain
T_r	Exciter Time Constant
K_c	Capacitor Control Gain
T_c	Capacitor Control Time Constant
x_q	Quadrature Axis Reactance
$x_q^{'}$	Quadrature Axis Transient Reactance
x_d	Direct Axis Reactance
$x_d^{'}$	Direct Axis Transient Reactance
r_l, x_l	Transmission Line Impedance
r_e, x_e	Shunt Transformer Impedance
r_b, x_b	Series Transformer Impedance
I_{ed}, I_{eq}	Shunt Transformer Current (I_e), Direct and Quadrature Axis Component
I_{ld}, I_{lq}	Series Line Current (I_l), Direct and Quadrature Axis Component
v_d, v_q	Armature Voltage, Direct and Quadrature Axis Component
V_b	Infinite Busbar Voltage
d_e	Shunt Converter Phase Angle
m_e	Amplitude Modulation index for shunt converter
d_b	Series Converter Phase Angle
m_b	Amplitude Modulation Index for Series Converter

u_c	Capacitor Input Control
$\dot{u}_c$	Derivative of u_c
u_{pss}	Power System Stabilizer Input Control
Φ	Right Eigenvector
Ψ	Left Eigenvector

Abbreviations

AC	Alternative Current
DC	Direct Current
FACTS	Flexible AC Transmission System
SVC	Static VAR Compensator
TCSC	Thyristor Controlled Series Capacitor
STATCOM	Static Synchronous Compensator
SSSC	Static Synchronous Series Controller
UPFC	Unified Power Flow Controller
PID	Proportional- Integral- Derivative
PSS	Power System Stabilizer
GTO	Gate Turn-Off Thyristor
VSC	Voltage- Sourced Converter
SMIB	Single Machine Infinite Bus

THESIS ABSTRACT

Name:	**MOHAMMED ABDULRAOUF AL-GHAZWI**
Title:	**EVALUATION OF DAMPING CONTROLS OF A UNIFIED POWER FLOW CONTROLLER**
Degree:	**MASTER OF SCIENCE**
Major Field:	**ELECTRICAL ENGINEERING**
Date of Degree:	**JUNE 2009**

With its unique capability to control simultaneously the real and reactive power flows on a transmission line, as well as to regulate voltage at the bus where it is connected, the Unified Power Flow Controller (UPFC) has a potential to create a tremendous impact on power system stability. The UPFC can allow loading of the transmission lines close to their thermal limits, forcing the power to flow through the desired paths. This will give the power system operators much needed flexibility in order to satisfy the demands that the deregulated power system will impose. This thesis examines the 5^{th} UPFC controls variables, viz shunt converter voltage magnitude and phase angle, series converter voltage magnitude and phase angle, capacitor control and power system stabilizer have been also considered. The effectiveness of these six controls in damping improvement has been studied through singular value decomposition (SVD), Hankel singular value (HSV), residue calculation, pole placement technique and lead-lag calculation methods. Simulation studies have been made to substantiate the finding the various decomposition methods. It has been observed that the responses of shunt transformer phase angle input control provides very good damping properties out of the whole inputs controls followed by series converter voltage magnitude, power system stabilizer, shunt converter voltage magnitude, series converter phase angle, capacitor control respectively.

Keywords: UPFC, FACTS, HSV, SVD, Residue, Pole Placement, Lead-Lag, Stabilizing compensator controller

Master of Science Degree

King Fahd University of Petroleum & Minerals, Dhahran.

JUNE 2009

ملخص الرسالة

إسم الطالب : محمد عبدالرؤوف محمد آل غزوي

عنوان الرسالة : تقييم تحكم الذبذبات من خلال سيطرة التدفق الكهربائي الموحد (UPFC)

التخصص : هندسة كهربائية

تاريخ التخرج : يونيو / 2009 م

بقابليته الفريدة للسيطرة على التدفق الكهربائي الحقيقي والتفاعلي في خطوط نقل الطاقة بالإضافة الى تنظيم الفلوتية عند نقطة التوصيل، فإن جهاز سيطرة التدفق الكهربائي الموحد (UPFC) له الاستطاعة في خلق التأثير الكبير على استقرار النظام الكهربائي. فجهاز سيطرة التدفق الكهربائي الموحد يمكن ان يسمح لتحميل خطوط نقل الطاقة بالقرب من حدودها الحرارية ، كما انه يجبر التدفق خلال الطرق المطلوبة، وهذه تعطي المشغل الكهربائي أكثر مرونة لإرضاء الطلبات في النظام الكهربائي. في هذه الرسالة يتم بحث أنظمة تحكم سيطرة التدفق الكهربائي الموحدة الست، وهي مقدار فولتية محول مجزئ التيار الكهربائي مع الزاوية ، مقدار فولتية محول على التوالي مع الزاوية ، تحكم مكثف وكذلك مثبت النظام. تم دراسة فعاليات المتغيرات الست من خلال تفسخ القيمة المفردة (SVD) ، قيمة Hankel المفردة (HSV) ، طريقة حساب البقية ، تقنية تحديد قطب ، واخيرا طرق حساب تأخر رئيسية . تم دراسة جميع أدوات التحكم الست لإيجاد الافضل منها وقد لوحظ بأن ردود محول الزاوية مجزئ التيار الكهربائي جيد جداً للسيطرة تلى ذلك مقدار الفولتية محول على التوالي، مثبت النظام الكهربائي، مقدار فولتية محول مجزئ التيار الكهربائي ، محول الزاوية على التوالي وأخيرا سيطرة المكثف.

الكلمات المفتاحية : UPFC ، FACTS ، HSV ، SVD ، البقية ، قطب التنسيب ، طرق التأخير

CHAPTER 1

INTRODUCTION

1.1 POWER SYSTEM STABILITY

A power system is an interconnection of generating units to load centers through high voltage electric transmission lines and, in general, is mechanically controlled. Electric power demand continues to grow and building of the new generating units and transmission circuits is becoming more difficult because of economic and environmental reasons. Therefore, power utilities are forced to depend on better utilization of existing generating units and to load the existing transmission lines close to their thermal limits. The power system should operate effectively without reduction in the system security and quality of supply even in the case of contingency conditions, to avoid system instability and possible black-outs. The examples of contingency conditions are losses of transmission lines and/or generating units, which occur frequently, and will most probably occur at a higher frequency under deregulation and major line or load switching. Under

the disturbance or contingency conditions the system could be poorly damped or even negatively damped giving rise to system oscillations and evenly transiently unstable situations.

A good power system should possess the ability to regain its normal operating condition after a disturbance. Since ability to supply uninterrupted electricity determines the quality of electric power supplied to the load, stability is regarded as one of the important topics of power system research [1, 2, 3].

Power system stability can be defined by the ability of synchronous machines to remain in synchronism with each other. The capability of power system to remain in synchronism in the event of possible disturbance such as line faults, generator and line outages and load switching etc., is characterized by its stability. Depending on the order of magnitude and type of disturbances, power system stability can be classified as steady state stability, transient stability and slowly growing stability [4, 5, 6].

Following unbalances in the system, a power system may experience sustained oscillations. These oscillations may be local to a single generator or they may involve a number of generators widely separated geographically (inter-area oscillations). Local oscillations can occur, for example, when a fast exciter is used on the generator. Inter area oscillations may appear as the system loading is increased across the weak transmission links. If not controlled, these oscillations may lead to partial or total power interruption [7, 8, 9].

Damping the oscillations is not only important in increasing the transmission capability but also for stabilization of power system conditions after critical faults. If the net damping of the system is negative, then the system may lose synchronism. Extra damping has to be provided to the system in order to avoid this. Powerful damping in the system has a two fold advantage of both decreasing the amplitude of first swing and the ratio of each successive swing to the preceding one, thus resulting in overall improvement of stability margin of the system [10, 11].

The major methods of damping of power system oscillations are:

1. Governor control: Control of input power P_m can stabilize a power system following a disturbance. Though governor control has shown some good results in damping control, it is not accepted by power utilities.

2. Excitation control: Among the various methods of damping, excitation control is one of the most common and economical method. Excitation controllers are referred to as power system stabilizers (*PSS*). Power system stabilizers have been thought to improve power system damping by generator voltage regulation depending on system dynamic response [12, 13].

3. Braking Resistors: Braking resistors prevent transient instability by immediately absorbing the real power that would otherwise be used in accelerating the generator. These are very effective to damp the first power system swing.

4. Control of the rotor angle (d): The electrical power output P_e can also be altered by varying the angle$d$. Phase shifters can be employed to perform this job.

5. Load shedding: This is the least considered option and is adopted as a last measure.

6. Control of the line reactance: The electrical power output can be controlled by controlling the line reactance. Reactance control can be achieved by series or shunt compensation. Traditionally fixed compensators have been switched in and out of the system mechanically at slow rates. Developments in power electronics have allowed dynamic control of these static shunt and series compensators.

In the late 1980s the Electric Power Research Institute (EPRI) has introduced a new technology program known as Flexible AC Transmission System (FACTS) [14]. The FACTS devices can be utilized in the existing power system by replacing mechanical controllers by reliable and high speed power electronic devices. In addition to steady state control of real and reactive flows in the system, the FACTS devices are known to be capable of improving the dynamic performance.

1.2 FACTS DEVICES

With the rapid development of power electronics, *Flexible AC Transmission Systems* (FACTS) devices have been proposed and implemented in power systems. FACTS devices can be utilized to control power flow and enhance system stability. Particularly

with the deregulation of the electricity market, there is an increasing interest in using FACTS devices in the operation and control of power systems with new loading and power flow conditions.

1.2.1 DEFINITION OF FACTS

According to IEEE, FACTS, which is the abbreviation of Flexible AC Transmission System, is defined as follows [16]:

Alternating current transmission systems incorporating power electronics based and other static controllers to enhance controllability and power transfer capability.

FACTS devices can be classified into the following.

1.2.2 FIRST GENERATION OF FACTS DEVICES

Power electronics based controllers were in use in power systems before N.G.Hingornani's use of the terminology, FACTS. These first generation FACTS devices have a common characteristic that is the necessary reactive power required for the compensation is generated or absorbed by traditional capacitor or reactor banks, and thyristor switches are used for control of the combined reactive impedance and these banks present to the system during successive periods of voltage application.

Consequently, conventional thyristor controlled compensator present a variable reactive admittance to the transmission network [22, 23].

Some of the first generation FACTS devices are,

1- Thyristor switched series capacitor (TSSC): A capacitive reactance compensator which consists of series capacitor bank shunted by a thyristor switched reactor to provide a stepwise control of series capacitive reactance.

2- Thyristor controlled series capacitor (TCSC): A capacitive reactance compensator which consists of a series capacitive bank shunted by a thyristor controlled reactor in order to provide smooth variation of series capacitive reactance.

3- Thyristor switched capacitor (TSC): Consists of a thyristor switched capacitor whose effective reactance is varied in stepwise manner by a thyristor valve. It is a shunt connected device.

1.2.3 SECOND GENERATION OF FACTS DEVICES

The second generation of FACTS controllers is based on voltage source converter, which use turn off devices like GTOs. These controllers require lower ratings of passive elements (inductors and capacitors) and the voltage source characteristics present several advantages over conventional variable impedance controllers.

Some of the FACTS controllers belonging to this category are

1. Static synchronous series compensator (SSSC): It is a voltage –sourced converter based series compensator and was proposed by Gyugi [22] in 1989.

2. Static synchronous compensator (STATCOM): STATCOM, previously known as STATCON or static condenser, is an advanced static Var compensator (SVC) using voltage source converters with capacitors connected on DC side.

STATCOM resembles in many respects a rotating synchronous condenser used for voltage control and reactive power compensation. As compared to conventional SVC, STATCOM does not require expensive large inductors, moreover it can also operate as reactive power sink or source flexibly, which makes STATCOM more attractive [24]. Because of its several advantages over conventional SVC, it is expected to play a major role in the optimum and secure operation of AC transmission system in future.

3. Unified power flow controller (UPFC): UPFC concept was proposed by Gyugi [22]. It consists of back to back voltage source converter arrangement, one converter of the back to back arrangement is in series and other is in shunt with the transmission line.

1.3 UNIFIED POWER FLOW CONTROLLER (UPFC) FOR IMPROVING STABILITY

The unified power flow controller (UPFC) is a FACTS device which can control power-system parameters such as terminal voltage, line impedance and phase angle [14, 17]. The primary function of the UPFC is to control power flow on a given line and voltage at the UPFC bus. This is achieved by regulating the controllable parameters of the system: line impedance, phase angle and voltage magnitude independently or simultaneously in any appropriate combinations. The UPFC can also be having the capabilities of controlling power flow in the transmission line, improving the transient stability, mitigation system oscillations and providing voltage support be utilized for damping power system oscillations by judiciously applying a damping controller.

1.4 THESIS OBJECTIVES

A good amount of work has been reported in the literature regarding the damping controls of UPFC. However, a systematic search in determining the hierarchy of the stabilizing control is very limited. Sometimes, the findings are even confusing.

This research examines the order of the various damping controls through several decomposition techniques. The procedure to achieve the thesis objective is broken down to the following steps:

1- Develop a dynamic model of a single machine infinite bus model including the UPFC.

2- Identify the various UPFC controls which can provide damping to the system.

3- Determination of the hierarchy of the UPFC controls by using different decomposition methods like singular value decomposition (SVD), residue method, and Hankel singular value (HSV).

4- Designing UPFC controllers using the residue, pole placement and power oscillation damping (POD) methods.

5- Realize the design using Lead-Lag and PI controllers.

6- Dynamic simulation for testing the controller design.

1.5 THESIS ORGANIZATION

This thesis is organized as follows: in Chapter 2, literature search on FACTS devices and their basic operating principles are presented.

Chapter 3 develops dynamic models of power system including UPFC for a single machine infinite bus system.

Chapter 4 presents some techniques used in the controllers design process. These controls are singular value decomposition, Hankel singular value, and residue.

The controller structures lead-lag compensators and PI controller are presented in chapter 5, while simulation studies for all controls are discussed in chapter 6

Finally, a conclusions and suggested future work are presented in chapter 7.

CHAPTER 2

LITERATURE SURVEY

This chapter presents a comprehensive literature search on FACTS Devices – introduction and these basic operating principles of FACTS devices are carried out. UPFC basic operation and characteristics are identified.

2.1 OPPORTUNITIES FOR FACTS

FACTS technology opens up new opportunities for controlling power and enhancing the usable capacity of present, as well as new and upgraded lines. The possibility that current through a line can be controlled at a reasonable cost enables a large potential of increasing the capacity of existing lines with larger conductors, and use of one of the FACTS

controllers to enable corresponding power to flow through such lines under normal and contingency conditions.

These opportunities arise through the ability of FACTS controllers to control the interrelated parameters that govern the operation of transmission systems including series impedance, shunt impedance, current, voltage, phase angle and the damping of oscillations at various frequencies below the rated frequency. These constraints cannot be overcome, while maintaining the required system reliability, by mechanical means without lowering the usable transmission capacity. By providing added flexibility, FACTS controllers can enable a line to carry power closer to its thermal rating. Mechanical switching needs to be supplemented by rapid response power electronics. It must be emphasized that FACTS is an enabling technology, and not a one-to-one substitute for mechanical switches.

The FACTS technology is not a single high power controller, but rather a collection of controllers, which can be applied individually or in coordination with others to control one or more of the interrelated system parameters mentioned above [18, 19, 20, 21].
Some of the functions of FACTS devices are,

• Regulation of power flows in prescribed transmission routes.

• Secure loadings of lines near their thermal limits.

• Prevention of cascading outages by contributing to emergency control.

• Damping of oscillations which can threaten security or limit the usable line capacity and improve system stability in general.

Below the different main types of FACTS devices are described:

2.1.1 STATIC VAR COMPENSATOR (SVC).

The most important FACTS devices have been used for a number of years to improve transmission line economics by resolving dynamic voltage problems. The accuracy, availability and fast response enable SVC's to provide high performance steady state and transient voltage control compared with classical shunt compensation. SVC's are also used to dampen power swings, improve transient stability, and reduce system losses by optimized reactive power control.

2.1.2 THYRISTOR CONTROLLED SERIES COMPENSATOR (TCSC)

TCSCs are an extension of conventional series capacitors through adding a thyristor-controlled reactor. Placing a controlled reactor in parallel with a series capacitor enables a continuous and rapidly variable series compensation system. The main benefits of TCSCs are increased energy transfer, dampening of power oscillations, dampening of subsynchronous resonances, and control of line power flow.

2.1.3 STATCOM

STATCOMs are GTO (gate turn-off type thyristor) based SVC's. Compared with conventional SVC's (see above) they don't require large inductive and capacitive

components to provide inductive or capacitive reactive power to high voltage transmission systems. This results in smaller land requirements. An additional advantage is the higher reactive output at low system voltages where a STATCOM can be considered as a current source independent from the system voltage.

2.1.4 UNIFIED POWER FLOW CONTROLLER (UPFC)

A special arrangement of two VSCs, one connected in series with the AC system and the other one connected in shunt, with common DC terminals is called Unified Power Flow Controller (UPFC). UPFC can be used for power flow control, loop flow control, load sharing among parallel corridors, providing voltage support, enhancement of transient stability, mitigation of system oscillations, etc.[14,16]. It can control all three basic power transfer parameters independently or simultaneously in any appropriate combinations. The UPFC can independently control real and reactive power flow along the transmission line at its output end, while providing reactive power support to the transmission line at its input end by regulating the DC-link capacitor voltage and varying both the phase angle and the modulation index of the input inverter [15]. This proposal addresses the dynamic performance enhancement impact of UPFC.

2.2 POSSIBLE BENEFITS FROM FACTS TECHNOLOGY

Within the basic system security guidelines, the FACTS devices enable the transmission system to obtain one or more of the following benefits [16, 25-28]:

- Control of power flow as ordered. This is the main function of FACTS devices. The use of power flow control may be to follow a contract, meet the utilities' own needs, ensure optimum power flow, ride through emergency conditions, or a combination of them.

- Increase utilization of lowest cost generation. One of the principal reasons for transmission interconnections is to utilize the lowest cost generation. When this cannot be done, it follows that there is not enough cost-effective transmission capacity. Cost-effective enhancement of capacity will therefore allow increased use of lowest cost generation.

- Dynamic stability enhancement. This FACTS additional function includes the transient stability improvement, power oscillation damping and voltage stability control.

- Increase the loading capability of lines to their thermal capabilities, including short term and seasonal demands.

- Provide secure tie-line connections to neighboring utilities and regions thereby decreasing overall generation reserve requirements on both sides.

- Upgrade of transmission lines.

- Reduce reactive power flows, thus allowing the lines to carry more active power.
- Loop flows control.

Table 1 describe the technical benefits of the principal FACTS devices. For each problem the conventional solution (e.g. shunt reactor or shunt capacitor) also can be used. For dynamic applications of FACTS in addressing problems in transient stability, dampening, post contingency voltage control and voltage stability. FACTS devices are required when there is a need to respond to dynamic (fast-changing) network conditions. The conventional solutions are normally less expensive than FACTS devices – but limited in their dynamic behavior. It is the task of the planners to identify the most economic solution.

	Load Flow Control	Voltage Control	Transient Stability	Dynamic Stability
SVC	●	●●●	●	●●
STATCOM	●	●●●	●●	●●
TCSC	●●	●	●●●	●●
UPFC	●●●	●●●	●●	●●

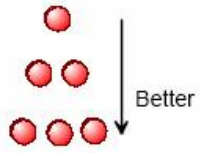

Table 1: Technical benefits of the main FACTS devices

2.3 UPFC BASIC OPERATION AND CHARACTERSTICS

This section will explain basic operation and characteristics of the UPFC. Since UPFC consists of two voltage-sourced converters (VSCs), basics of VSCs will be briefly discussed at the beginning of the section.

2.3.1 BASICS OF VOLTAGE SOURCE CONVERTERS AND PULSE WIDTH MODULATION TECHNIQUE

Typical three-phase VSC is shown in Figure 2.1

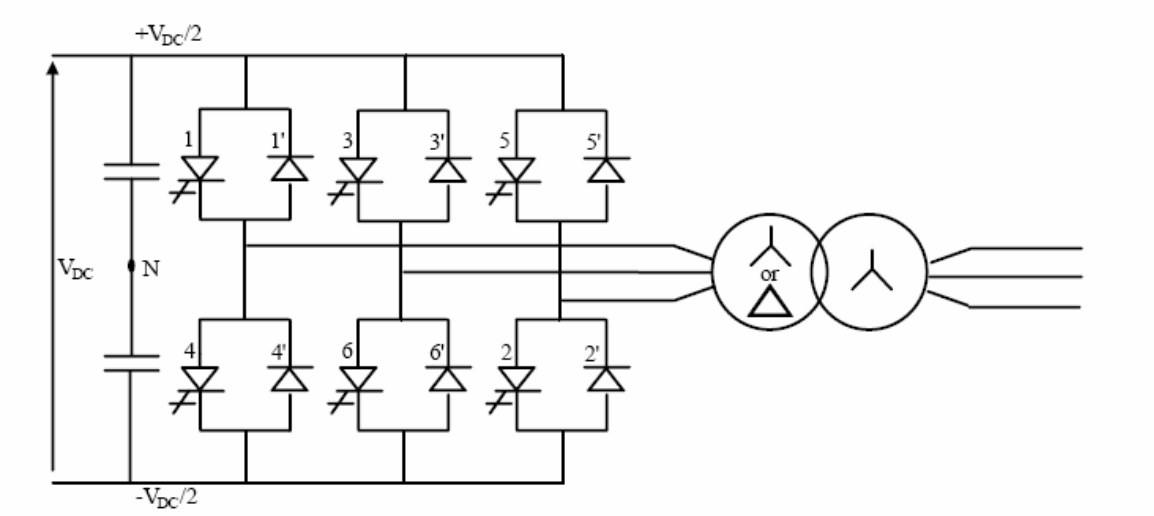

Figure 2.1 Three-phase voltage sourced-converters

It is made of six valves each consisting of a gate turn off device (GTO) paralleled with a reverse diode, and a DC capacitor. An AC voltage is generated from a DC voltage through sequential switching of the GTOs. The DC voltage is unipolar and the DC current can flow in either direction.

Controlling the angle of the converter output voltage with respect to the AC system voltage controls the real power exchange between the converter and the AC system. The real power flows from the DC side to AC side (inverter operation) if the converter output voltage is controlled to lead the AC system voltage. If the converter output voltage is made to lag the AC system voltage the real power will flow from the AC side to DC side

(rectifier operation). Inverter action is carried out by the GTOs while the rectifier action is carried out by the diodes. Two switches on the same leg cannot be on at the same time.

Controlling the magnitude of the converter output voltage controls the reactive power exchange between the converter and the AC system. The converter generates reactive power for the AC system if the magnitude of the converter output voltage is greater than the magnitude of the AC system voltage. If the magnitude of the converter output voltage is less than that of the AC system the converter will absorb reactive power.

The converter output voltage can be controlled using various control techniques. Pulse Width Modulation (PWM) techniques can be designed for the lowest harmonic content. It should be mentioned that these techniques require large number of switching per cycle leading to higher converter losses. Therefore, PWM techniques are currently considered unpractical for high voltage applications. However, it is expected that recent developments on power electronic switches will allow practical use of PWM controls on such applications in the near future. Due to their simplicity many authors, i.e. [29, 30, 31, 32], have used PWM control techniques in their UPFC studies.

2.3.2 UPFC DESCRIPTION AND OPERATION

The basic components of the UPFC are two voltage source converters sharing a common DC storage capacitor, and connected to the system through coupling transformers. The voltage source at the sending bus is connected in shunt and will therefore be called the shunt voltage source. The second source, the series voltage source, is placed between the

sending and the receiving busses. The UPFC is placed on high-voltage transmission lines. This arrangement requires step-down transformers in order to allow the use of power electronics devices for the UPFC. A basic UPFC functional scheme is shown in Figure 2.2.

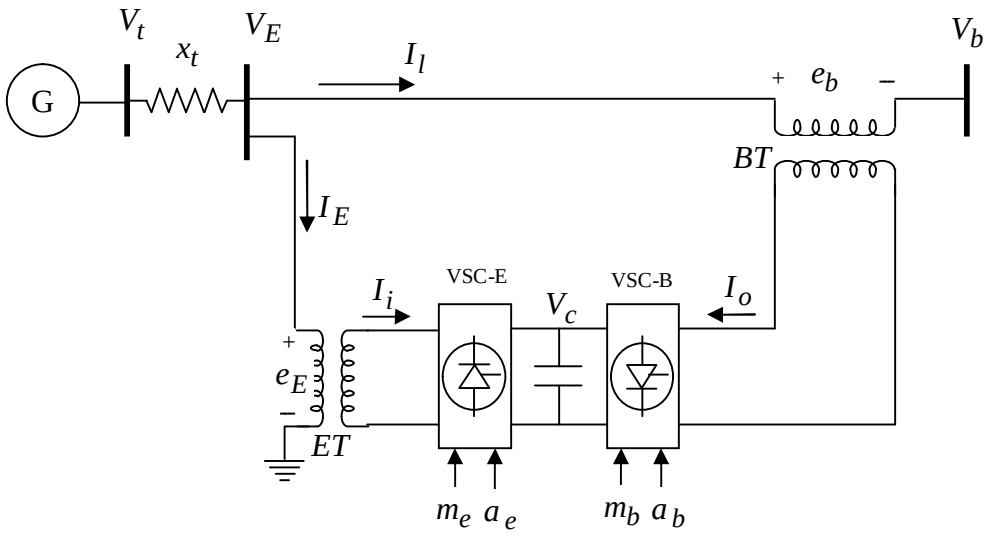

Figure 2.2 Power system with UPFC

The series converter is controlled to inject a symmetrical three phase voltage system, vse, of controllable magnitude and phase angle in series with the line to control active and reactive power flows on the transmission line. So, this converter will exchange active and reactive power with the line. The reactive power is electronically provided by the series converter, and the active power is transmitted to the DC terminals. The shunt converter is operated in such a way as to demand this DC terminal power (positive or negative) from the line keeping the voltage across the storage capacitor V_{dc} constant. So, the net real power absorbed from the line by the UPFC is equal only to the losses of the two

converters and their transformers. The remaining capacity of the shunt converter can be used to exchange reactive power with the line so to provide a voltage regulation at the connection point.

The two voltage source converters can work independently of each other by separating the DC side. So in that case, the shunt converter is operating as a STATCOM that generates or absorbs reactive power to regulate the voltage magnitude at the connection point. Instead, the series converter is operating as SSSC that generates or absorbs reactive power to regulate the current flow, and hence the powers flow on the transmission line.

Because of its attractive features, modeling and controlling an UPFC have come into intensive investigation in the recent years.

Several references in technical literature can be found on development of UPFC steady state, dynamic and linearized models. Steady state model referred as an injection model is described in [33].

If a UPFC is operated in the automatic control mode (i.e. to maintain a pre-specified power flow between two power system buses, the sending and the receiving buses, and to regulate the sending end voltage at the specific value) the UPFC sending end is transformed into a PV bus while the receiving end is transformed into a PQ bus, and conventional load flow (LF) program can be performed [29]. This method is simple and easy to implement but it will only work if real and reactive power flows and the sending bus voltage magnitude are controlled simultaneously. It should be also mentioned that

there is no need for an iterative procedure used in [29] to compute UPFC control parameters. They can be computed directly after the conventional LF solution is found. Due to the advantages that the automatic power flow control mode offers, this mode will be used as the basic operation mode for the most of the practical applications.

A Newton-Rhapson based algorithm for large power systems with embedded FACTS devices is derived in [45]. In [46] this algorithm was extended to include UPFC application. It allows simultaneous or independent control of real and reactive powers and voltage magnitude. The algorithm itself is very complicated and hard to implement. It considerably increases the order of the Jacobian matrix in the iterative procedure and is quite sensitive to initial condition settings. Improper selection of initial condition can cause the solution to oscillate or diverge.

UPFC dynamic model known as a fundamental frequency model can be found in [29, 32, 49, 53]. This model consists of two voltage sources one connected in series and the other one in shunt with the power network to represent the series and the shunt voltage source inverters. Both voltage sources are modeled to inject voltages of fundamental power system frequency only. Model in [49] neglects the DC link capacitor dynamics which might make results obtained using this model inaccurate, models in [29, 32, 53] include DC link capacitor dynamics and can be used for study of UPFC effect on the real power system behavior.

The linearized model of the power network including UPFC is useful for small signal analysis and damping controller design. The UPFC linearized model can be found in [49] and [52]. While deriving these models some simplification have been made, i.e. the model described in [49] does not include DC link dynamics, the model derived in [52] assumes that the UPFC sending and receiving buses are also generator terminal buses. However, UPFC can be connected between any two buses in the network. Therefore, these models do not represent the general form of the linearized network.

General form of the linearized model of the network with UPFC included will be derived in the case study of this thesis.

2.4 UPFC POWER OSCILLATION DAMPING CONTROLLER DESIGN

In this section, Linear method for UPFC power oscillation damping controller design will be discussed. Generally, there are two kinds of power oscillation damping controllers in power systems: power system stabilizer and FACTS power oscillation damping controllers. Power system stabilizer acts through the excitation system of generator to increase the damping of electromechanical oscillations by generating a component of electrical torque proportional to speed change.

Usually power system stabilizers are designed for damping local electromechanical oscillations. However, in large power systems, these power system stabilizers may not provide enough damping for inter-area modes. In this case, FACTS devices offer an effective strategy for inter-area modes damping control.

UPFC power oscillation damping controller design generally, the damping function of UPFC devices is performed mainly through the changes of the power delivered along the transmission line. With appropriate lead-lag compensation, the damping torque provided by the UPFC damping control is proportional to the gain of the controller.

Since UPFC device is located in transmission systems, local input signals are always preferable. Residue method, singular value decomposition (SVD), Hankel singular value (HSV) and damping torque components are an appropriate approach in finding the most proper local feedback signal in the controller design procedure. Moreover, it is also a simple and practical approach for designing of UPFC power oscillation damping controllers. Therefore, in this thesis, residue method, singular value decomposition (SVD), and Hankel singular value (HSV) are applied and the linear UPFC power oscillation damping controller design procedure is shown as follows:

- Selection of proper feedback signal.
- Design of the controller using the above method.
- Test the controller under operation condition.

CHAPTER 3

POWER SYSTEM MODEL WITH UPFC

Power system analysis requires proper and adequate mathematical representation so as to include all significant components of the power system. Dynamic models, both non-linear and linearized, for single machine infinite bus installed with UPFC are presented in this chapter.

3.1 THE SINGLE MACHINE INFINITE BUS SYSTEM

A single machine infinite bus (SMIB) system including the UPFC is shown in Figure 3.1. The UPFC is composed of an excitation transformer (*ET*), a boosting transformer (*BT*), two three-phase GTO based voltage source converters (VSC), and a DC link capacitor. Symbols 'm'and 'a'refer to amplitude modulation index and phase angle of the control

signal of the two VSCs (*E* and *B*), respectively which can be adjusted through their own control loops.

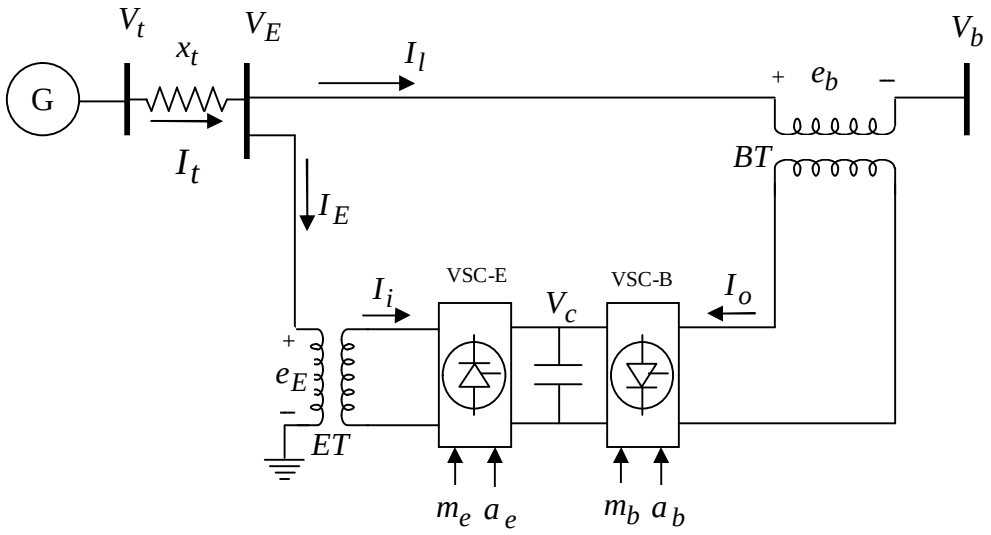

Figure 3.1 UPFC installed in SMIB power system

The dynamic models for the various components of the system are given in the following sections.

3.1.1 SYNCHRONOUS GENERATOR AND ITS EXCITATION SYSTEM

The synchronous generator is modeled through a 3rd order dynamic including the q-axis component of transient voltage and electromechanical swing equation representing motion of the rotor. The internal voltage equation of the generator is written as,

$$\dot{e}_q' = \frac{1}{T_{do}'}[E_{fd} - e_{qo}' - (x_d - x_d')I_d] \qquad (3.1)$$

where, $e_q^{'}$ subscript *d* and *q* represents the direct and quadrature axis of the machine. $x_d, x_d^{'}$, and $T_{do}^{'}$ are the d-axis synchronous reactance, transient reactance and open circuit field constants, respectively. I_d is the current along the d-axis and $e_q^{'}$ is the voltage behind the transient reactance.

The electromechanical swing equation is broken into two first order differential equations and is written as,

$$\dot{w}^{'} = \frac{1}{2H}[P_m - P_e - D(w-1)]$$
$$d^{'} = w_b(w-1) \qquad (3.2)$$

where, the electrical power output is,

$$P_e = v_d I_d + v_q I_q$$
$$v_d = x_q I_q$$
$$v_q = e_q^{'} - x_d^{'} I_d$$

v_d and v_q are components of generator terminal voltage (V_t). P_m is the mechanical power input. H is the inertia constant in seconds, (2H = M). w_b is the synchronous speed. x_q and $x_d^{'}$ are quadrature axis synchronous reactance and transient reactance.

The IEEE type ST is used for the voltage regulator excitation. The block diagram of the excitation system is shown in Figure 3.2.

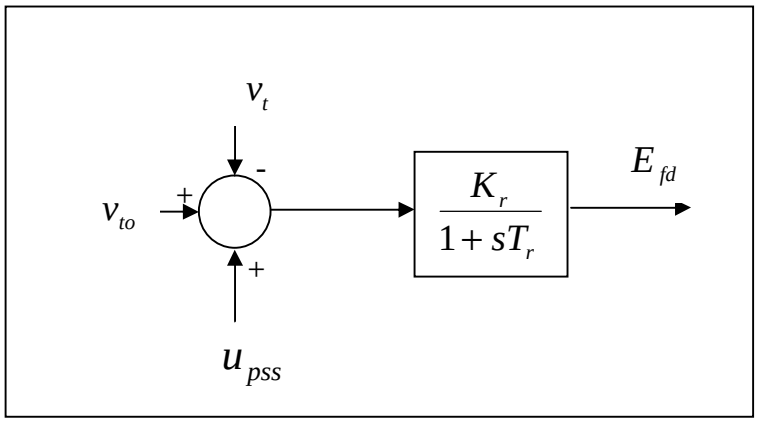

Figure 3.2 Block diagram of excitation system

The dynamic model of the excitation system is,

$$E'_{fd} = \frac{K_r}{T_r}[v_{to} - v_t + u_{pss}] - \frac{E_{fd}}{T_r} \tag{3.3}$$

where, K_r and T_r are the gain and time constant of exciter, respectively. v_{to} represents the steady state (reference) value of terminal voltage. u_{pss} is the power system stabilizer input control.

3.1.2 THE UPFC SYSTEM

In the power system model shown in Figure 3.1 V_E and V_b are the generator terminal voltage and infinite bus bar voltage, respectively. The total current drawn from the

sending end I_t consists of the current flowing through the line I_l and the current exchanged with the shunt converter I_E of the UPFC system. Shunt transformer inductance and resistance are represented by L_e and r_e. Series transformer inductance and resistance are assumed negligible compared to transmission line impedance.

By performing Park transformation, the current through the shunt inverter can be described by the following equations

$$\frac{dI_{ed}}{dt} = -w_o \frac{r_e}{L_e} I_{ed} + w_o(1+w) I_{eq} + \frac{w_o}{L_e}(v_{ed} - e_{ed})$$
$$\frac{dI_{eq}}{dt} = -w_o \frac{r_e}{L_e} I_{eq} - w_o(1+w) I_{ed} + \frac{w_o}{L_e}(v_{eq} - e_{eq}) \quad (3.4)$$

where subscripts *d* and *q* denote the Park components of the currents and voltages. Similarly, the transmission line can be described by

$$\frac{dI_{ld}}{dt} = -w_o \frac{r_l}{L_l} I_{ld} + w_o(1+w) I_{lq} + \frac{w_o}{L_l}(v_{ed} - v_{bd} - e_{bd})$$
$$\frac{dI_{lq}}{dt} = -w_o \frac{r_l}{L_l} I_{lq} - w_o(1+w) I_{ld} + \frac{w_o}{L_l}(v_{eq} - v_{bq} - e_{bq}) \quad (3.5)$$

where,

$$v_{ed} = (x_q + x_t)(I_{eq} + I_{lq}) \quad (3.6)$$

$$v_{eq} = e'_{eq} - (x'_d + x_t)(I_{ed} + I_{ld})$$

$$v_{bd} = v_b \cos(d_{e_q} - d_{v_b})$$

$$v_{bq} = v_b \sin(d_{e_q} - d_{v_b}) \tag{3.7}$$

$$e_{ed} = m_e V_c \cos a_e$$

$$e_{eq} = m_e V_c \sin a_e \tag{3.8}$$

$$e_{bd} = m_b V_c \cos a_b$$

$$e_{bq} = m_b V_c \sin a_b \tag{3.9}$$

where,

x_q and x_t are quadrature axis synchronous reactance and transformer reactance connected to the generator bus respectively. I_{eq} and I_{lq} are quadrature of shunt transformer and the transmission line current, I_{ed} and I_{ld} are direct of shunt transformer and the transmission line current, m_e and a_e are the modulation index and angle of shunt converter. V_c is DC-link capacitor voltage.

The instantaneous powers at the AC and DC terminals of the input and output converters are equal if the converters are assumed to be lossless.

$$C\frac{dV_c}{dt} = (I_i + I_o) \tag{3.10}$$

This gives two power balance equations in per unit,

$$V_c I_i = e_{ed} I_{ed} + e_{eq} I_{eq}$$

$$V_c I_o = e_{bd} I_{ld} + e_{bq} I_{lq} \tag{3.11}$$

(3.9) and (3.11) substituted in (3.10) gives,

$$\frac{dv_c}{dt} = \frac{1}{C}[m_e I_{ed} \cos a_e + m_e I_{eq} \sin a_e + m_b I_{ld} \cos a_b + m_b I_{lq} \sin a_b] \tag{3.12}$$

A new idea which has not been reported in the literature is to change the capacitance (*C*) of the UPFC system. This can be achieved in a similar way as static var control (SVC) system. The impact of varying *C* on the system performance has been examined. Figure 3.3 shows the block diagram of the controller. An auxiliary control u_c in the circuit can adjust the susceptance *B* of the UPFC DC capacitor to cater for the system need.

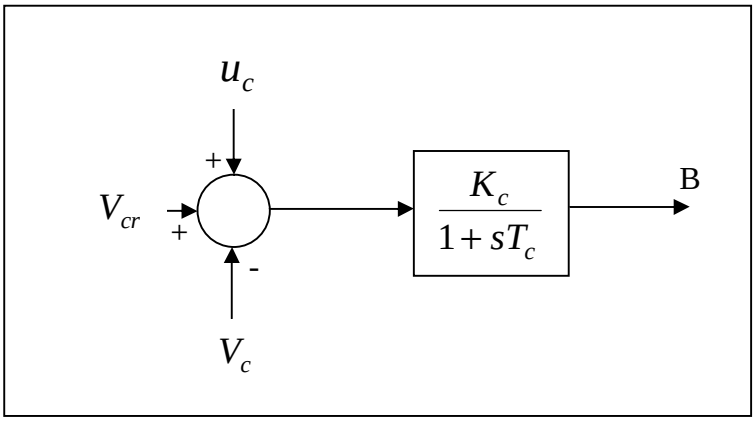

Figure 3.3 Block diagram of capacitor control

The dynamic model of the capacitor control drive is given below:

$$\frac{B}{(V_{cr}-V_c)+u_c}=\frac{K_c}{1+sT_c}$$

$$\Delta B+T_c\Delta\dot{B}=K_c(V_{cr}-V_c+u_c)$$

$$\Delta\dot{B}=\frac{K_c}{T_c}(-\Delta V_c+u_c)-\frac{1}{T_c}\Delta B$$

$$\Rightarrow\quad \frac{dB}{dt}=-\frac{1}{T_c}[K_c\Delta v_c+B]+\frac{K_c}{T_c}u_c \qquad (3.13)$$

where, K_c and T_c are the gain and time constant of capacitor control circuit, respectively. In the above, V_{cr} represents the steady state (reference) value of voltage.

The composite model of a synchronous generator UPFC system can be expressed through the 10th nonlinear dynamic equations,

$$\frac{dI_{ed}}{dt} = -w_o \frac{r_e}{L_e} I_{ed} + w_o(1+w) I_{eq} + \frac{w_o}{L_e}(v_{ed} - e_{ed})$$

$$\frac{dI_{eq}}{dt} = -w_o \frac{r_e}{L_e} I_{eq} - w_o(1+w) I_{ed} + \frac{w_o}{L_e}(v_{eq} - e_{eq})$$

$$\frac{dI_{ld}}{dt} = -w_o \frac{r_l}{L_l} I_{ld} + w_o(1+w) I_{lq} + \frac{w_o}{L_l}(v_{ed} - v_{bd} - e_{bd})$$

$$\frac{dI_{lq}}{dt} = -w_o \frac{r_l}{L_l} I_{lq} - w_o(1+w) I_{ld} + \frac{w_o}{L_l}(v_{eq} - v_{bq} - e_{bq})$$

$$\frac{dB}{dt} = -\frac{1}{T_c}[K_c \Delta v_c + B] + \frac{K_c}{T_c} u_c$$

$$\frac{dv_c}{dt} = \frac{1}{C + \frac{dB}{dt}}[m_e I_{ed} \cos a_e + m_e I_{eq} \sin a_e + m_b I_{ld} \cos a_b + m_b I_{lq} \sin a_b]$$

$$\frac{dd}{dt} = w_o w$$

$$\frac{dw}{dt} = \frac{1}{2H}[P_m - P_e - Dw]$$

$$\frac{de_q^{'}}{dt} = \frac{1}{T_{do}^{'}}[E_{fd} - e_{qo}^{'} - (x_d - x_d^{'})I_d]$$

$$\frac{dE_{fd}}{dt} = \frac{K_r}{T_r}[v_{to} - v_t + u_{pss}] - \frac{E_{fd}}{T_r}$$

These can be expressed in terms of the non-linear state equations

$$\dot{x} = f(x,u) \qquad (3.14)$$

where x is the vector of the states $[I_{ed}, I_{eq}, I_{ld}, I_{lq}, B, V_c, d, w, e_q^{'}, E_{fd}]^T$

and control vector u is $[m_e, a_e, m_b, a_b, u_c, u_{pss}]^T$.

3.2 THE LINEARIZED EQUATIONS

The nonlinear set of equations (3.1), (3.2), (3.3), (3.4), (3.5), (3.12) and (3.13) can be linearized around a nominal operating point and can be expressed as

$$sI_{ed} = -w_o \frac{r_e}{L_e}\Delta I_{ed} + w_o(1+w)\Delta I_{eq} + \frac{w_o}{L_e}(\Delta v_{ed} - \Delta e_{ed}) \qquad (3.15)$$

$$sI_{eq} = -w_o \frac{r_e}{L_e} \Delta I_{eq} - w_o(1+w)\Delta I_{ed} - w_o I_{ed} \Delta w + \frac{w_o}{L_e}(\Delta v_{eq} - \Delta e_{eq})$$

(3.16)

$$sI_{ld} = -w_o \frac{r_l}{L_i} \Delta I_{ld} + w_o(1+w)\Delta I_{lq} + \frac{w_o}{L_i}(\Delta v_{ed} - \Delta v_{bd} - \Delta e_{bd}) \quad (3.17)$$

$$sI_{lq} = -w_o \frac{r_l}{L_i} \Delta I_{lq} - w_o(1+w)\Delta I_{ld} + \frac{w_o}{L_i}(\Delta v_{eq} - \Delta v_{bq} - \Delta e_{bq}) \quad (3.18)$$

$$sB = -\frac{1}{T_c}[K_c \Delta v_c + \Delta B] + \frac{K_c}{T_c} \Delta u_c \quad (3.19)$$

$$sV_c = \frac{1}{C + \Delta B}[\Delta I_o + \Delta I_i] \quad (3.20)$$

$$s\,\Delta d = w_o \Delta w \quad (3.21)$$

$$sw = \frac{1}{2H}(-T_e - D\Delta w) \quad (3.22)$$

$$se_q^{'} = \frac{1}{T_{do}^{'}}[\Delta E_{fd} - \Delta e_{qo}^{'} - (x_d - x_d^{'})(\Delta I_{ed} + \Delta I_{ld}) \quad (3.23)$$

$$sE_{fd} = -\frac{K_r}{T_r}\Delta v_t + \frac{K_r}{T_r}\Delta u_{pss} - \frac{1}{T_r}\Delta E_{fd} \tag{3.24}$$

where,

$$\Delta v_{ed} = (x_q + x_t)(\Delta I_{eq} + \Delta I_{lq}) \tag{3.25}$$

$$\Delta e_{ed} = m_e \cos a_e \Delta V_c - m_e \sin a_e V_c \Delta a_e + \Delta m_e \cos a_e V_c \tag{3.26}$$

$$\Delta v_{eq} = \Delta e'_{eq} - (x'_d + x_t)(\Delta I_{ed} + \Delta I_{ld}) \tag{3.27}$$

$$\Delta e_{eq} = m_e \sin a_e \Delta V_c + m_e \cos a_e V_c \Delta a_e + \Delta m_e \sin a_e V_c \tag{3.28}$$

$$\Delta v_{bd} = v_b \cos(d_{e_q} - d_{v_b})\Delta d \tag{3.29}$$

$$\Delta e_{bd} = m_b \cos a_b \Delta V_c - m_b \sin a_b V_c \Delta a_b + \Delta m_b \cos a_b V_c \tag{3.30}$$

$$\Delta v_{bq} = v_b \sin(d_{e_q} - d_{v_b})\Delta d \tag{3.31}$$

$$\Delta e_{bq} = m_b \sin a_b \Delta V_c + m_b \cos a_b V_c \Delta a_b + \Delta m_b \sin a_b V_c \tag{3.32}$$

$$\Delta I_o = m_e[\cos(a_e)\Delta I_{ed} + \sin(a_e)\Delta I_{eq}] + [I_{ed}\cos(a_e) + I_{eq}\sin(a_e)]\Delta m_e - [I_{ed}\sin(a_e) - I_{eq}\cos(a_e)]m_e\Delta a_e \quad (3.33)$$

$$\Delta I_i = m_b[\cos(a_b)\Delta I_{ld} + \sin(a_b)\Delta I_{lq}] + [I_{ld}\cos(a_b) + I_{lq}\sin(a_b)]\Delta m_b - [I_{ld}\sin(a_b) - I_{lq}\cos(a_b)]m_b\Delta a_b \quad (3.34)$$

$$\Delta v_t = -\frac{v_{qo}}{v_{to}}x_d^{'}\Delta I_{ed} + \frac{v_{do}}{v_{to}}x_q\Delta I_{eq} - \frac{v_{qo}}{v_{to}}x_d^{'}\Delta I_{ld} + \frac{v_{do}}{v_{to}}x_q\Delta I_{lq} + \frac{v_{qo}}{v_{to}}\Delta e_q^{'} \quad (3.35)$$

Arranging the state equations in matrix form gives the linear state matrix equations

$$\dot{x} = Ax + Bu \quad (3.36)$$

Here, (x) is the perturbation of the states and (u) is the vector of control. Details of the derivations are given in Appendix A.

CHAPTER 4

DETERMINATION OF HIERARCHY OF THE UPFC DAMPING CONTROLS

The six controls variables [$m_e, a_e, m_b, a_b, u_c, u_{pss}$] identified in previous chapter are evaluated in terms of their effectiveness in terms of providing damping to the system. The methods employed for the evaluation processes are singular value decomposition (SVD), Hankel singular value (HSV), and residue method. These methods are briefly outlined in the following sections.

4.1 SINGULAR VALUE DECOMPOSITION (SVD)

To measure the controllability of the electromechanical mode by a given input, the singular value decomposition (SVD) is a useful tool. Mathematically, if *G* is an *m*×*n* complex matrix then there exist unitary matrices *W* and *V* with dimensions of *m*×*m* and *n*×*n* respectively such that *G* can be written as

$$G = W \sum V^H \qquad (4.1)$$

where

$\sum = \begin{bmatrix} \sum_1 & 0 \\ 0 & 0 \end{bmatrix}$; this is m×n matrix and $\sum_1$ is defined as

$$\sum_1 = \begin{bmatrix} s_1 & 0 & . & 0 \\ 0 & s_2 & . & 0 \\ . & . & . & . \\ 0 & 0 & 0 & s_r \end{bmatrix}$$

where $r = min\{m,n\}$ and $s_1 \geq s_2 \geq \ldots . \geq s_r \geq 0$ are placed diagonally in a descending order and s_i^2 is an eigenvalue of $G^H G$, where G^H is the complex conjugate transpose of *G*.

The minimum singular value, $s_{\min}$, of the matrix [λI–*A bi*] indicates the capability of the i^{th} input to control the mode associated with the eigenvalue (l) . In this study, the matrix *B* can be written as *B* = [*b*1, *b*2, *b*3, *b*4, *b*5, *b*6] where *bi* is the column of matrix *B* corresponding to the i^{th} input. As a matter of fact, the higher the $s_{\min}$, the higher the

controllability of this mode by the input considered. Having been identified, the controllability of the electromechanical mode can be examined with all inputs in order to identify the most effective one to control that mode [36]. For the single machine infinite bus power system considered, the *A* and *B* matrices in (3.16) are given in appendix B. These are calculated for a loading of 1.02 p.u. The parameters of the system and steady state operating values of other variables for this loading condition are included in Appendix F.

For 10 state variables and 6 control inputs, the dimensions of matrices *A* and *B* are 10×10 and 10×6 respectively. The eigenvalues of the A matrix for nominal operation are [-28 ±j2790.3, -9.4 ±j377.5, -21.8, -19.7, -0.2 ±j4.0, -0.3 ±j0.8]

The singular value decomposition method was used for the SMIB linearized model. The minimum singular values corresponding to all the 6^{th} control variables for a range of operating conditions were computed. The results have been plotted in Figure 4.1. From the plot it can be observed that the ranks in terms of $s_{\min}$ are shunt transformer phase angle followed by power system stabilizer, shunt transformer voltage magnitude, series transformer voltage magnitude, series transformer phase angle and capacitor control respectively. This implies that input a_e, the shunt converter phase angle control, has the highest controllability of oscillation mode.

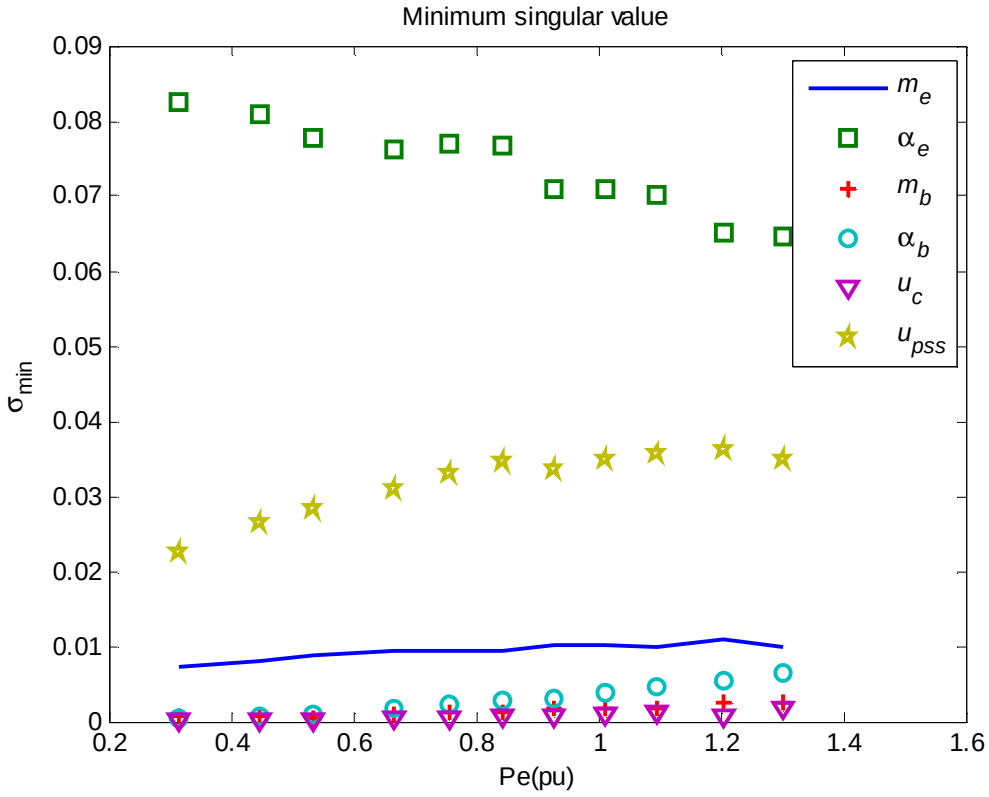

Figure 4.1: Minimum singular value output

4.2 HANKEL SINGULAR VALUES (HSV)

Controllability and observability of a system play an important role in selecting input-output signals. In order to specify which combination of input-output contains more information about the system internal states, one possible approach is to evaluate observability and controllability indexes of the system.

A system is said to be controllable if for any initial state $\Delta x\ (t_0) = x_0$ and any final state $\Delta x(t_1) = x_1$, there exists an input that transfers x_0 to x_1 in a finite time. Otherwise, the system is said to be uncontrollable.

The system is said to be observable if for any unknown initial state $\Delta x\ (t_0\ ) = x_0$, there exists a finite $t_1 > 0$ such that the knowledge of the input u and output y over $[0, t_1]$ suffices to determine uniquely the initial state x_0. Otherwise, the system is said to be unobservable.

A linear time invariant system can be defined as

$$G = \begin{cases} \dot{x} = Ax + Bu \\ y = Cx + Du \end{cases} \qquad (4.2)$$

Two possible ways to check that the above system is controllable are

• (A, B) is controllable if and only if matrix f , defined as

$f = [B \ \ AB \ \ A^2B \ \ \ldots\ldots \ \ A^{n-1}B]$ has full rank n, where n is the number of states.

• (A, B) is controllable if and only if the controllability Gramian matrix defined as

$$P = \int_0^\infty e^{At} BB^T e^{A^T t} dt \tag{4.3}$$

is positive definite, which has full rank n . Matrix P is the solution to the following Lyapunov equation:

$$AP + PA^T + BB^T = 0 \tag{4.4}$$

Also, there are two possible ways to check the observability of the above system:

• (A ,C) is observable if and only if matrix y , defined as

$$y = \begin{bmatrix} C \\ CA \\ . \\ CA^{n-1} \end{bmatrix} \text{ has full rank n.} \tag{4.5}$$

• (A ,C) is observable if and only if the observability Gramian matrix defined as

$$Q = \int_0^\infty e^{A^T t} CC^T e^{At} dt \tag{4.6}$$

has full rank n and, thus, is positive definite.

Matrix *Q* satisfies the following Lyapunov equation:

$$A^T Q + QA + C^T C = 0 \qquad (4.7)$$

P and *Q* are symmetric and since the realization is minimal they are also positive definite. The eigenvalues of the product of the controllability and observability gramians play an important role in system theory and control. We define the Hankel singular values, s_i, as the square roots of the eigenvalues of *PQ*

$$s_i = \sqrt{l_i(PQ)} \quad \text{i=1,…..,n} \qquad (4.8)$$

which reflects the joint controllability and observability of the states of a system where $l_i(PQ)$ is i^{th} the eigenvalue of PQ .

Thus, for choosing input and output signals, the HSV can be calculated for each combination of inputs and outputs, the candidate with the largest HSV shows better controllability and observability properties. It means that this candidate can give more information about system internal states [36].

Figure 4.2 shows the representation of Hankel singular value s_i against the 10 eigenvalues corresponding to the 10 states. It can be observed the largest singular value is for the shunt converter phase angle followed in order, series converter voltage magnitude

(m_b), power system stabilizer (u_{pss}), shunt converter voltage magnitude (m_e), series converter phase angle(a_b), capacitor control (u_c) respectively. This again indicates the shunt converter phase angle was the highest controllability of oscillation mode.

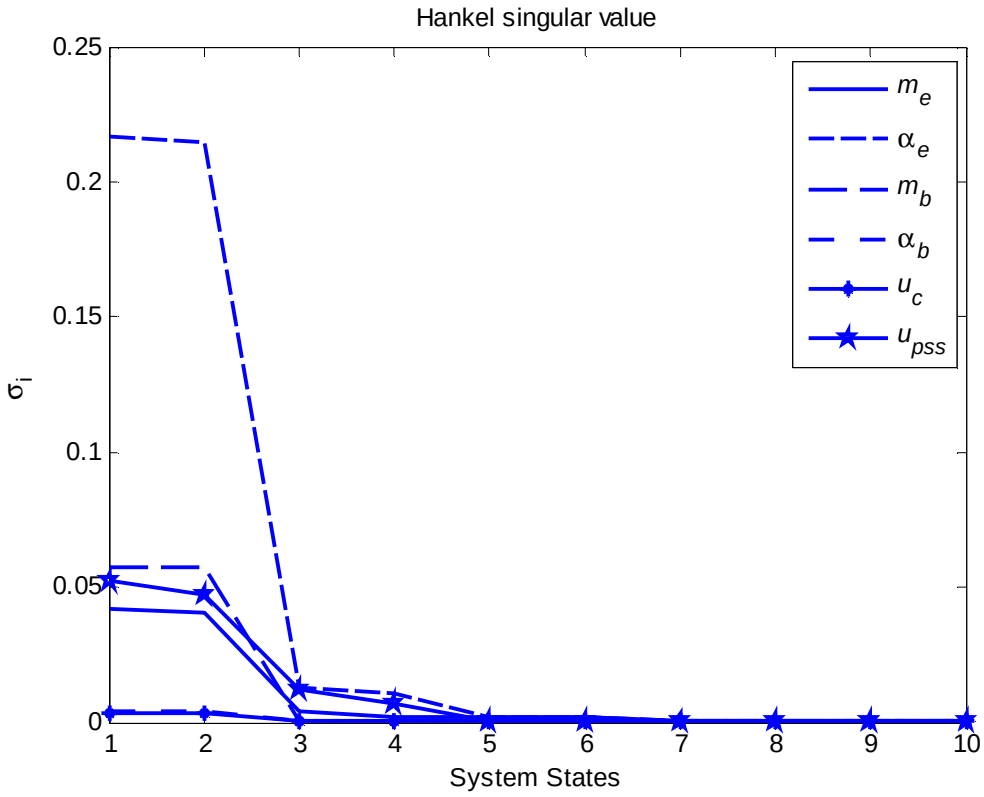

Figure 4.2: Hankel singular value output

4.3 RESIDUE METHOD

Choosing an appropriate output variable, the state-output system of equations for UPFC device can be represented by following equation:

$$\Delta \dot{X} = A\Delta x + B\Delta u \qquad (4.9)$$
$$\Delta y = C\Delta x + D\Delta u$$

where

$\Delta \dot{x}$ is the state vector (dimension 10× 1)

Δu is the input vector (dimension 6 × 1)

Δy is the output vector (dimension 1 × 1)

A is the state matrix (dimension 10 × 10)

B is the input matrix (dimension 10× 6)

C is the output matrix (dimension 1 × 10)

D is the feed forward matrix

The eigenvalues of matrix *"A"* are given by

$$\det(A - lI) = 0 \tag{4.10}$$

Expansion of the determinant gives the characteristic equation. The n_x solutions of $l = l_1,.....,l_{n_x}$ are eigenvalues of *A*.

Let $l_i = s_i \pm jw_i$

Be the i^{th} eigenvalue of the state matrix *A*. The real part of the eigenvalues gives the damping, and the imaginary part gives the frequency of oscillation. The relative damping ratio is given by:

$$x = \frac{-s}{\sqrt{s^2 + w^2}} \tag{4.11}$$

The critical oscillatory modes considered here are those having damping ratio less than 3%.

If the state space matrix *A* has *n* distinct eigenvalues, Λ, Φ and Ψ below are the diagonal matrix of eigenvalues and matrices of right and left eigenvectors, respectively:

Any non-zero vector Φ_i which satisfies

$$A\Phi = \Phi\Lambda \tag{4.12}$$

is termed the right eigenvector of *A*, corresponding to the eigenvalue l_i . Φ_i has dimension $n_x \times 1$. The n_x right eigenvectors conform the modal matrix

$$\Phi = [\Phi_1 \quad \Phi_2 \quad \ldots \quad \Phi_{n_x}]_{n_x \times n_x}$$

Likewise, any non-zero vector "Ψ_i" which satisfies

$$\Psi A = \Lambda\Psi \tag{4.13}$$

is termed the left eigenvector of *A* corresponding to the eigenvalue l_i. Ψ_i has dimension $1 \times n_x$. The n_x left eigenvectors conform the modal matrix

$$\Psi = \left[(\Psi_1)^T \quad (\Psi_2)^T \quad \ldots\ldots \quad (\Psi_{n_x})^T\right]^T_{n_x \times n_x}$$

As a summery n_x eigenvalues can be expressed in the following matrix form

$$A\Phi = \Phi\Lambda$$
$$\Psi A = \Lambda\Psi$$
$$\Psi = \Phi^{-1}$$

In order to modify a mode of oscillation by feedback, the chosen input must excite the mode and it must also be visible in the chosen output. The measures of those two properties are the controllability and observability, respectively. The modal controllability and modal observability matrices are defined as follows:

$$B' = \Phi^{-1}B$$
$$C' = C\Phi \qquad (4.14)$$

The mode is uncontrollable if the corresponding row of the matrix B' is zero. The mode is unobservable if the corresponding column of the matrix C' is zero. If a mode is either uncontrollable or unobservable, feedback between the output and the input will have no effect on the mode. The open loop transfer function of a SISO (single input single output) system is:

$$G(s) = \frac{y(s)}{u(s)} = C(sI - A)^{-1}B \qquad (4.15)$$

G(s) can be expanded in partial fractions of the Laplace transform of *y* in terms of *C*, *B*, matrices and the right and left eigenvectors as:

$$G(s) = \sum_{i=1}^{N} \frac{C\Phi(:,i)\Psi(i,:)B}{(s - l_i)} = \sum_{i=1}^{N} \frac{R_i}{(s - l_i)} \tag{4.16}$$

Each term in the denominator of the summation is a scalar called residue. The residue for a particular mode gives the sensitivity of that mode's eigenvalue to feedback between the output *y* and the input *u* for a SISO system. It is the product of the mode's observability and controllability.

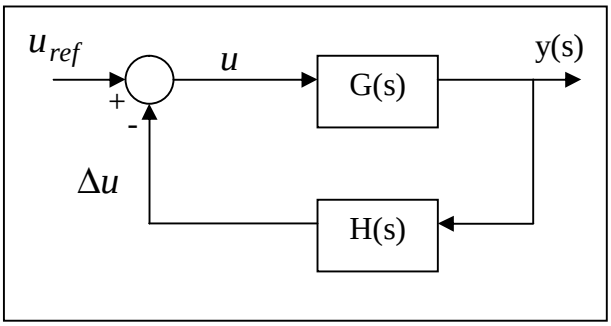

Figure 4.3: Feedback control system

Figure 4.3 shows a system G(s) equipped with a feedback control $H(s,k) = kH(s)$ where *k* is a constant gain between output and input, when applying the feedback control, eigenvalues of the initial system G(s) are changed. It can be proved [37], that when the feedback control is applied, movement of an eigenvalue is calculated by:

$$\frac{dl_i}{dk} = R_i H(l_i) \tag{4.17}$$

for small values of gain, the equation can be written as:

$$\frac{\Delta l_i}{\Delta k} = R_i H(l_i)$$

If a feedback transfer function is added to the open system, it can be shown that

$$\begin{aligned} \Delta l_i &= R_i H(l_i, k) \\ \Delta l_i &= k R_i H(l_i) \end{aligned} \tag{4.18}$$

It can be observed from (4.18) that the shift of the eigenvalue caused by a controller is proportional to the magnitude of the residue. The change of eigenvalue must be directed towards the left half complex plane for optimal damping improvement. For a certain mode to be controlled, a same type of feedback control *H(s)*, regardless of its structure and parameters, is tried out at different locations. For the mode of the interest, the residues at tried locations are calculated. The largest residue indicates the most effective location to apply the feedback control.

Figure 4.4 shows a plot of the residues of the SMIB power system against system eigenvalues (or states). The output of the system considered to be speed deviation giving

the *C* matrix to be [0 0 0 0 0 0 0 1 0 0]. For the values of *A* and *B* matrices for the nominal operating point the plant transfer function was computed as

$$G(s) = \sum_{i=1}^{N} \frac{C\Phi(:,i)\Psi(i,:)B}{(s - l_i)} = \sum_{i=1}^{N} \frac{R_i}{(s - l_i)}$$

where Φ and Ψ are obtained through (4.12) and (4.13).

From Figure 4.4 we can observe that 1, 2, 7 and 8 contribute the largest residue and hence are most controllable and observable. We exclude 1, 2 because they correspond to stator currents of the generator. States 7 and 8 correspond to the electromechanical modes of oscillation. The residue indices indicate that control of shunt converter angle will be most effective in terms of damping control of the system, following in order by series converter voltage magnitude (m_b), power system stabilizer (u_{pss}), shunt converter voltage magnitude (m_e), series converter phase angle(a_b), capacitor control (u_c) respectively.

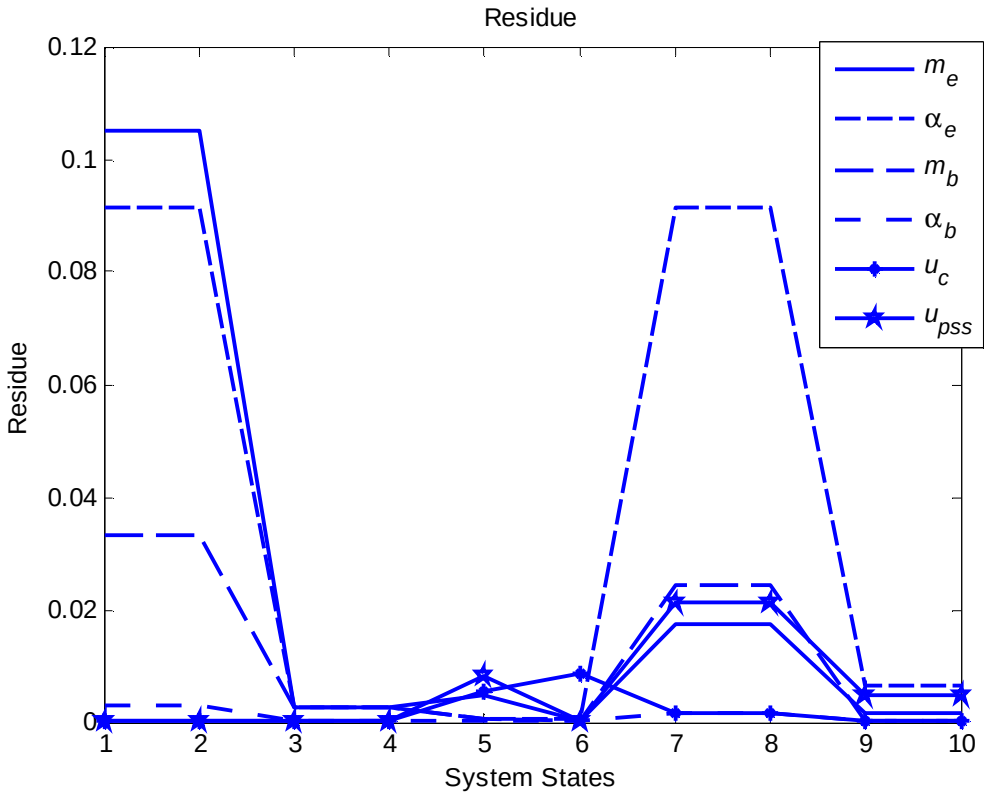

Figure 4.4: Residue output plot

4.4 THE HIERARCHY OF DAMPING CONTROL

The three methods presented in these sections, viz the minimum singular value, Hankel singular value and residue methods, give the similar hierarchy of the damping controls. Only the singular value method indicate the PSS to be the second best. Again, if we compare the indices one with another, all the 3 methods indicate greater superiority of the shunt converter phase angle control. Since in an actual power system not all the controls will be applied at the same time, shunt converter phase angle control may be an appropriate choice.

CHAPTER 5

CONTROLLER STRUCTURES

Once the effectiveness of the six controls variables [$m_e, a_e, m_b, a_b, u_c, u_{pss}$] in terms of providing the damping to the system is determined, the next step is to design the controllers which will appropriately modulate the control signals. The controller structures used in this thesis are lead-lag compensators and PI controls. Here, we note that PI controllers are special case of lead-lag. The methods utilized in determing the gains and time constants of these circuits are based on

- Residue principle
- Power oscillation damping (POD)
- Pole placement

5.1 LEAD-LAG COMPENSATOR

The lead-lag controllers are used in power system to produce an electrical torque in phase with the speed deviation providing a additional damping to the system. The control of the UPFC can be modulated through auxiliary circuits in order to produce these damping torques. The outputs deviation of generator speed Δw is considered as the input to these controllers. The six alternative UPFC based damping controls are examined in the present work.

The transfer function of a lead-lag block and in power system analysis is shown in Figure 5.1

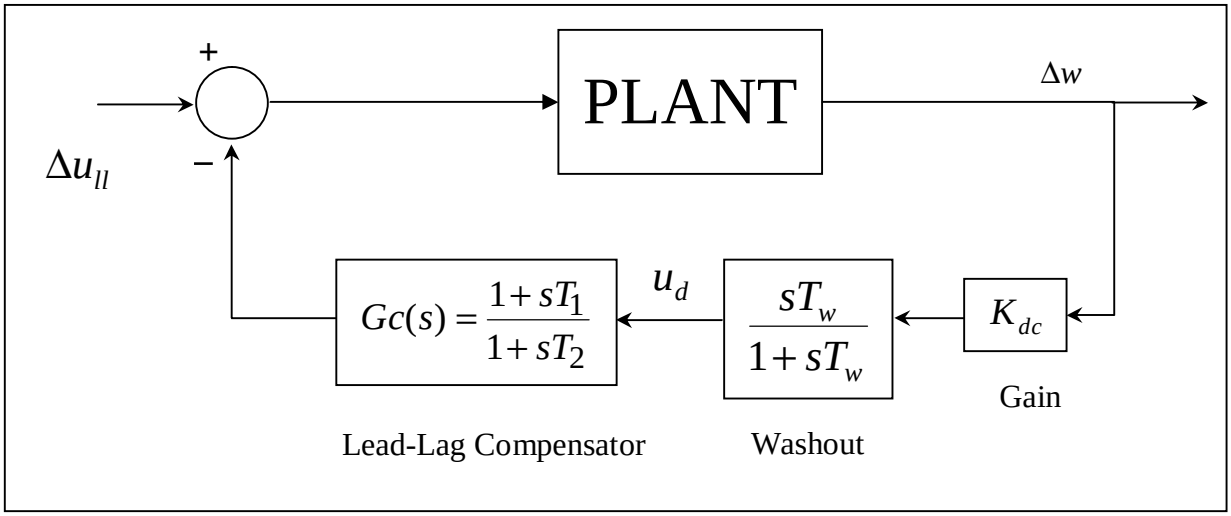

Figure 5.1 Block diagram for lead-lag system

The additional control circuit in the feedback path consists of washout block in cascade with the lead-lag circuit. The parameters of the damping controller T_1, T_2 and K_{dc} are obtained by using the damping controller design. The value of the washout time constant T_w should be high enough to allow signals associated with oscillations in rotor speed to

pass unchanged. From the viewpoint of the washout function, the value of T_w is not critical and may be in the range of 1s to 20s. The detailed step-by-step procedure for computing the parameters of the damping controllers using lead-lag compensation technique is given below [5]:

1. Computation of natural frequency of oscillation w_n from the mechanical loop.

$$w_n = \sqrt{\frac{k_1 w_o}{M}} \tag{5.1}$$

2. Computation of $\angle G_e$ (phase lag between Δu and ΔP_e) at $s = jw_n$; let it be g .

3. Design of phase lead/lag compensator G_c:

The phase lead/lag compensator G_c is designed to provide the required degree of lead-lag compensation. For 100% phase lead/lag compensation,

$$\angle G_c(jw_n) + \angle G_e(jw_n) = 0 \tag{5.2}$$

Assuming one lead-lag network,

$$T_1 = aT_2 \tag{5.3}$$

the transfer function of the phase lead/lag compensator becomes,

$$G_c(s) = \frac{1 + saT_2}{1 + sT_2} \tag{5.4}$$

Since the phase angle compensated by the lead-lag network is equal to - g the parameters *a* and T_2 are computed as,

$$a = \frac{1 + \sin g}{1 - \sin g} \tag{5.5}$$

$$T_2 = \frac{1}{w_n \sqrt{a}} \tag{5.6}$$

4. Computation of optimum gain K_{dc}.

The required gain setting K_{dc} for the desired value of damping ratio z is obtained as,

$$K_{dc} = \frac{2z w_n M}{|G_c(s)||G_e(s)|} \tag{5.7}$$

where $|G_c(s)|$ and $|G_e(s)|$ are evaluated at *s* = jw_n. The signal washout is the high pass filter that prevents steady changes in the speed from modifying the UPFC input parameter.

The combination of the compensator and washout will introduce 2 more differential equations [Y_u], which have to be solved along with 10 system differential equations

5.2 PI CONTROLLER.

Proportional-integral-derivative [PID] is one of the most widely used controllers in continuous data control systems. The function of the proportional control is to make the response faster. The function of the integral control is to reduce steady state error, whereas the derivative control provides an anticipatory action to reduce the overshoots in the response, stabilize the system and slow down transient behavior.

In order to get the best performance from a three-term controller, the amount of each action has to be selected carefully. *PID* control has been used in the industry because of its ease in use and it can be tuned to meet time domain specifications. In this section we will use residue method and pole placement techniques to determine the parameters of the *PI* controller.

5.2.1 DETERMINATION OF CONTROLLER GAIN THROUGH RESIDUE METHOD

The block diagram of transfer function of *PI* controller in the feedback path is shown in Figure 5.2

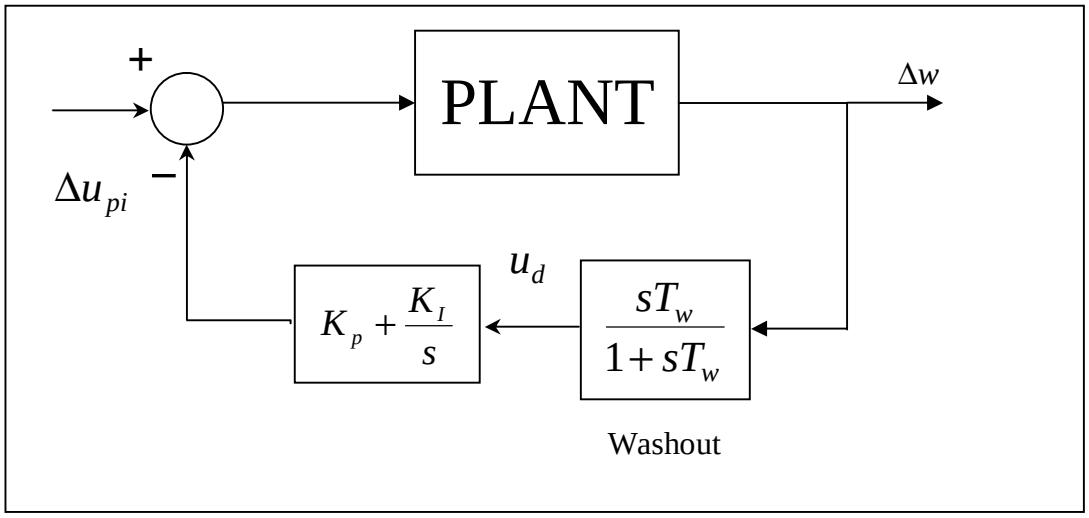

Figure 5.2 Block diagram for PI Controller

This consists of a washout in addition to the proportional integral (*PI*) blocks. The transfer functions of the controllers

$$H(s)=\left(\frac{sT_w}{1+sT_w}\right)\left(K_p+\frac{K_I}{s}\right)=kH_1(s) \tag{5.9}$$

where,

$$kH_1(s)=K_I\left[\frac{sT_w}{1+sT_w}\right]\left[\frac{1+T_3s}{s}\right] \tag{5.10}$$

$$T_3=\frac{K_p}{K_I} \tag{5.11}$$

The detailed step-by-step procedure for computing the parameters of the *PI* controller using the residue method is given in the follwing [5]:

1- For given *A*, *B*, and *C* matrices calculate R_i from the relation,

$$G(s)=\sum_{i=1}^{N}\frac{C\Phi(:,i)\Psi(i,:)B}{(s-l_i)}=\sum_{i=1}^{N}\frac{R_i}{(s-l_i)} \quad (5.12)$$

Identify the state corresponding to the largest residue. Note, Φ and Ψ for the different eigenvalues are obtained from equations (4.12) and (4.13).

2- Calculate the angle $\Phi_c = 180^0 - \arg(R_i)$ (5.13)

3- Find angle of line $-\frac{K_p}{K_I}$ from the trigonometric equality $\angle l_i - \Phi_c$. Call it Φ_{pole}.

4- We know, $\Phi_{pole} = \angle l_i + \frac{K_p}{K_I}$ (5.14)

5- Use the trigonometric relationship

$$\frac{\mathrm{Im}(l_i)}{\frac{K_I}{K_p}+real(l_i)}=\tan(\Phi_{pole}) \text{ and solve for } \frac{K_I}{K_p} \quad (5.15)$$

6- Use this value of $\frac{K_p}{K_I}$ in implementing the controller

Note, the addition of washout and *PI* control will introduce 2 differential equations in this case also, which will be integrated with system differential equations.

5.2.2 CONTROLLER DESIGN THROUGH POLE PLACEMENT CONTROL TECHNIQUE

One way of finding the parameters of the *PI* controller is the pole placement technique. In the design of fixed gain *PI* stabilizer, the gain settings K_p and K_I can be computed by assigning a pair of pre-specified eigenvalues $l = l_1$ and $l = l_2$ of the closed loop system of Figure 5.2. This is usually referred to as the pole-assignment or pole-placement method. The steps involved are:

1. Determine the poles of the uncompensated plant given by the system equations

$$\dot{x} = Ax + Bu$$
$$y = Cx \qquad (5.16)$$

2. Calculate the damping ratio (z) from the dominant (electromechanical mode) eigenvalues.

3. Determine how much to the left the eignvalues have to be shifted in order to get desired damping. Record the eignvalues $l_{1,2} = s \pm jw$

4. For the desired eignvalues, the closed loop system including the feedback controller H should satisfy the requirement that

$$\det[I - (lI)^{-1}BH(l)C] = 0$$

This yields,

$$H(l) = \frac{1}{C(lI - A)^{-1}B} \tag{5.17}$$

where,

$$H(l) = \frac{l}{1+l}\left(K_p + \frac{K_I}{l}\right) = \frac{lK_p}{1+l} + \frac{K_I}{1+l} \tag{5.18}$$

For $l = s + jw$, (5.15) and (5.16) yield

$$\begin{aligned} &\frac{s(s+1)+w^2}{(s+1)^2+w^2}K_p + \frac{(s+1)}{(s+1)^2+w^2}K_I = real\ part\ of\ H(l) \\ &\frac{w}{(s+1)^2+w^2}K_p - \frac{w}{(s+1)^2+w^2}K_I = imaginary\ part\ of\ H(l). \end{aligned} \tag{5.19}$$

The details are given in appendix D

The composite model of a synchronous generator UPFC system including the lead-lag or PI controller can be expressed through the 12th order dynamic relationship,

$$\dot{x} = f(x,u) \tag{5.20}$$

Here, the state vector $x = [\ I_{ed}, I_{eq}, I_{ld}, I_{lq}, B, V_c, d, w, e'_q, E_{fd}, x_{c1}, x_{c2}\ ]^T$ and the control (u) comprises of $[m_e, a_e, m_b, a_b, u_c, u_{pss}]^T$. The last two states are contributed by the controllers,

CHAPTER 6

SIMULATION STUDIES

The single machine infinite bus system given in Figure 3.1 was simulated to test the six UPFC controller identified in the previous chapters. As indicated in chapter 4, the parameters of the system are given in Appendix F. In the following, lag-lead and *PI* designs are implemented independently for the six controllers m_e, a_e, m_b, a_b, u_c and u_{pss} followed by coordinated application of the controls. All the comparative studies were made with the same disturbance of 10% torque pulse.

6.1 SIMULATION STUDIES WITH LEAD-LAG CONTROLLER

The lead-lag compensator designs were carried out through the procedure given in Chapter 5. The *POD* controller was implemented such that it compensates the phase lag

between the control input print and power output print in the system block diagram. The design parameters are T_1, T_2 and K_{dc} in Figure 5.1. The design was carried out for the following controls

- Shunt converter phase angle (a_e).
- Shunt converter voltage magnitude (m_e).
- Series converter phase angle (a_b).
- Series converter voltage magnitude (m_b).
- Power system stabilizer (u_{pss}).
- Capacitor control (u_c).

Table 6.1 list the parameters obtained through the design procedure presented, for all the controls listed.

Input Control	T_1	T_2	K_{dc}
a_e	1.0967	0.07	-4.1365
m_b	0.8091	0.09	-22.535
m_e	0.4567	0.15	36.4523
a_b	0.1699	0.4	-403.78
u_c	0.1521	0.45	-325.85
u_{pss}	1.0967	0.7	9.2937

Table 6.1: Optimum gain settings for lead-lag method

Figure 6.1 and 6.2 show the synchronous generator speed and rotor angle response following a 10% input torque pulse with and without the proposed lead-lag compensator. Responses are plotted for all the six controls. The response without control is oscillatory. While all the controls seem to provide reasonable damping, out of the 5 converter controls, the shunt converter phase angle control is slightly superior. While it is well known that in such scenarios, PSS control with a lead compensator is satisfactory, this serves as a basic for comparison. The variable capacitor control does not seem to be very promising, as was also observed in the decomposition method analysis.

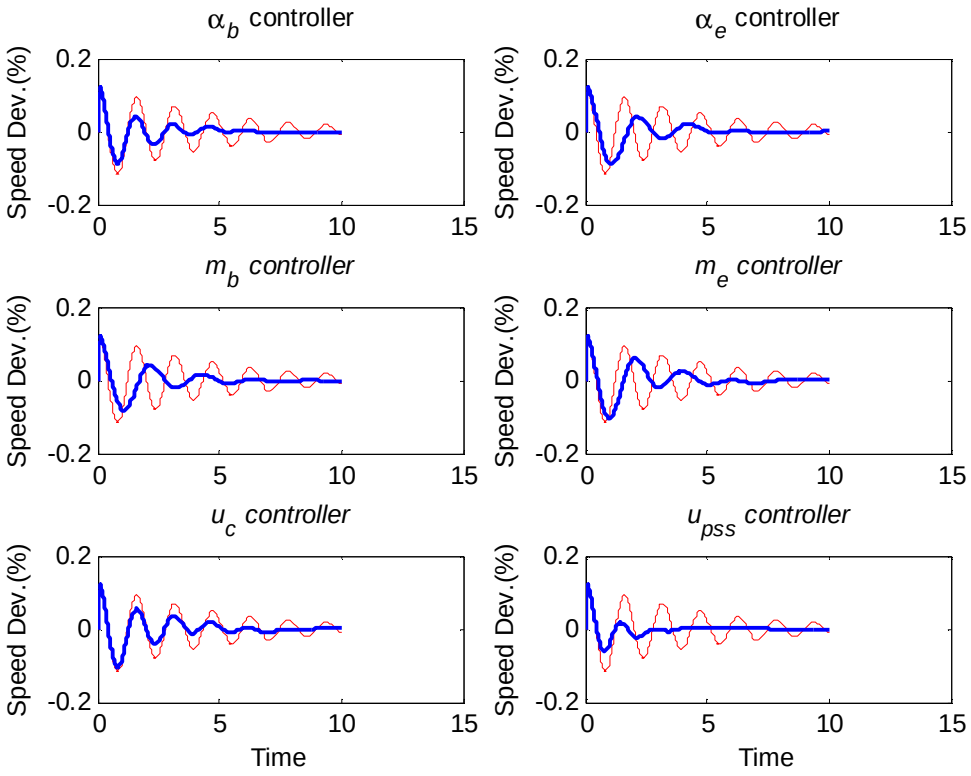

Figure 6.1: Generator speed variation with time following a 10% input torque pulse for 0.1 sec, with and without the lead-lag compensator

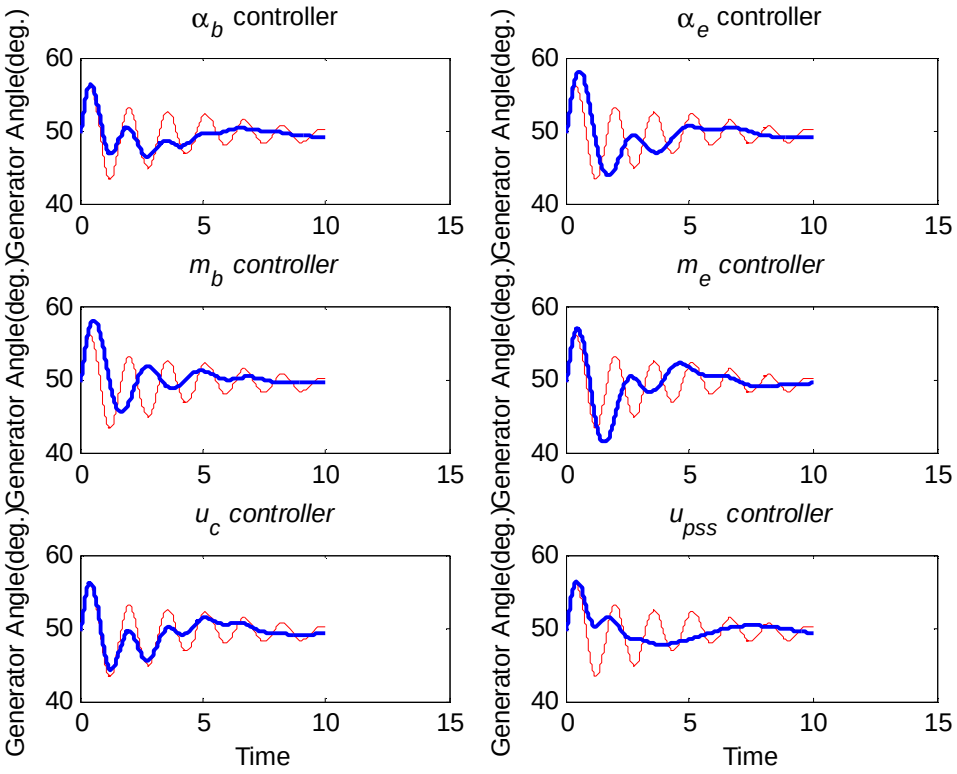

Figure 6.2: Generator rotor angle variation following a 10% torque pulse for 0.1 sec, with and without the lead-lag compensator

6.2 SIMULATION STUDIES WITH PI CONTROLLER

As mentioned earlier, the *PI* controller designs were carried out through the help of two techniques. These are residue method and by pole placement technique. In the residue method, the *PI* gain are so adjusted that the compensator controls the phase angle of the residue eventually improving the system transient behavior. The pole placement method is more direct, where *PI* gains are adjusted to give specific closed loop system damping ratio.

6.2.1 RESIDUE METHOD

The gains of the *PI* controller obtained through the residue calculations are tabulated in Table 6.2 for the various control inputs $a_e, m_e, m_b, \ldots\ldots$ etc. the corresponding damping ratio (z) are also shown. If we observe the damping ratio obtained through incorporation of different controls, it can be seen that all the 5 converter controls provide more or less equal and reasonable amount of damping. The damping ratio obtained with the PSS control, however, is not that satisfactory.

Input Control	z	K_p	K_I
a_e	0.2224	-7.4	1.9
m_b	0.2234	-28.58	-7.5
m_e	0.2241	36.56	60
a_b	0.2288	-455.11	-115
u_c	0.212	-391.48	-350
u_{pss}	0.1133	-1.963	-46

Table 6.2: Optimum gain settings for PI controller through residue method

The fact can be seen more clearly from the simulated transient responses shown in Figure 6.3 and 6.4. the speed deviations and angle with the 5 controls are more or less a like, while it is poor with the *PSS* control.

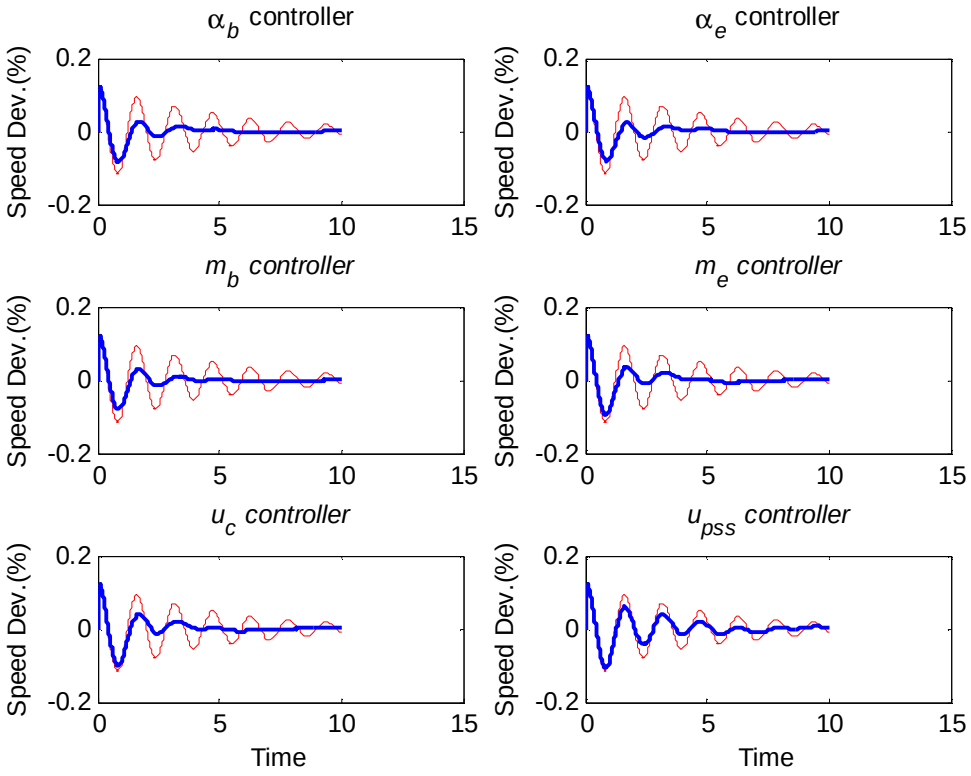

Figure 6.3: Generator speed variation with time following a 10% input torque pulse for 0.1 sec, with and without the residue PI controller

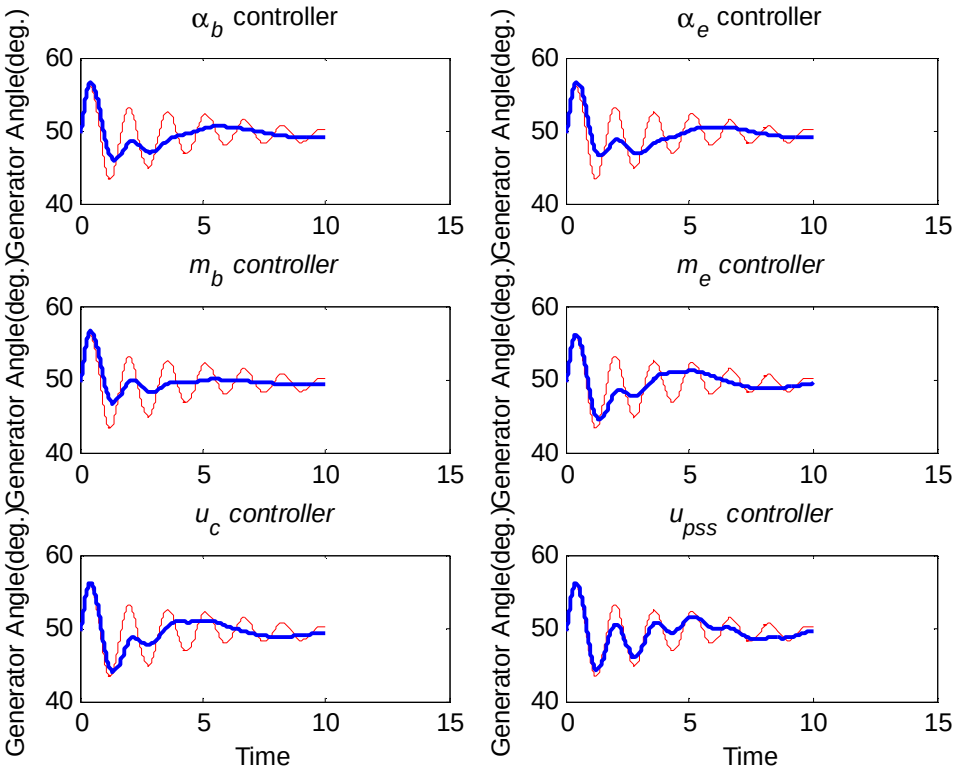

Figure 6.4: Generator rotor angle variation following a 10% torque pulse for 0.1 sec, with and without residue PI controller

6.2.2 POLE PLACEMENT TECHNIQUE

The eignvalues of the uncompensated system are [-28 ±j2790.3, -9.4 ±j377.5, -21.8, -19.7, -0.2 ±j4.0, -0.3 ±j0.8]. The corresponding damping factor find from the dominant eignvalues is -0.2 ±j4.0. In view of the fact that other methods gave a damping ratio of the order of 0.22, it was decided to design the *PI* controller such that the closed-loop system damping ratio is 0.22. The values of K_p and K_I obtained for the various control inputs are listed in Table 6.3.

Input Control	K_p	K_I
a_e	-8.3211	-7.9027
m_b	-30.29	-43.06
m_e	36.39	100.28
a_b	-472.3	-685.637
u_c	517.13	1075.9
u_{pss}	0.7633	-42.118

Table 6.3: Optimum gain settings for PI controller through pole placement

Figure 6.5 and 6.6 show the transient generator speed and angle variations with the different control inputs being generated through the *PI* controllers given in Table 6.3. Since the design closed loop damping ration is 0.22, it is generally expected that the transient responses in this figures will be similar. With the *PSS* control, however, it was observed that simulation gave a slight worsened response. The difference control have been in the inadequacy of the linear system to represent the nonlinear dynamics.

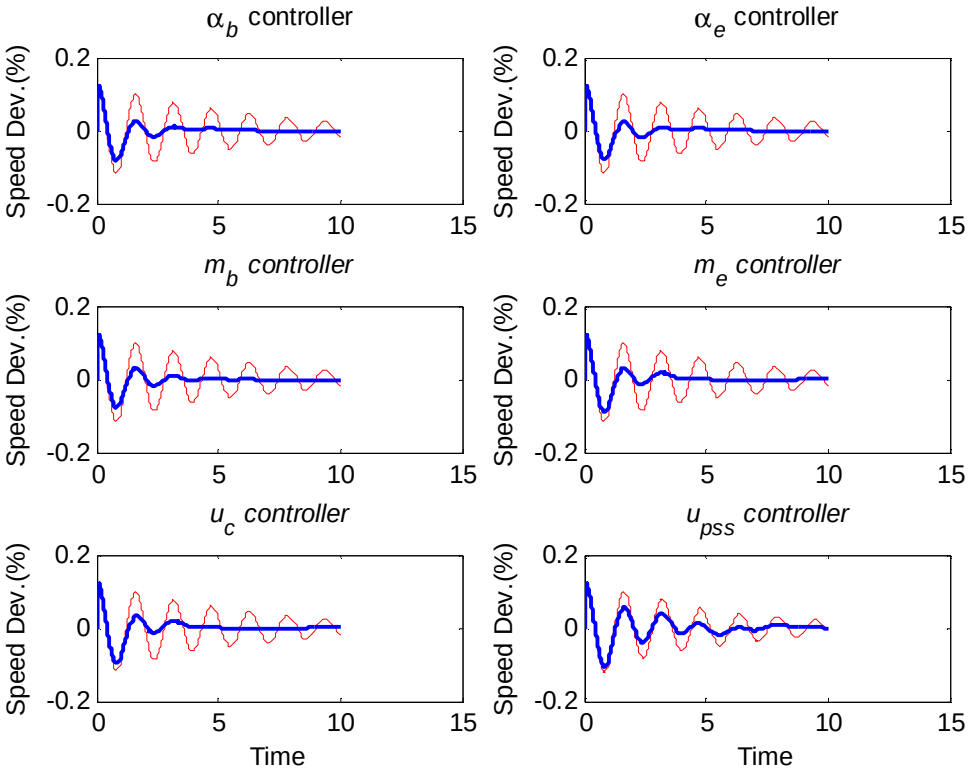

Figure 6.5: Generator speed variation with time following a 10% input torque pulse for 0.1 sec, with and without the PI pole placement method

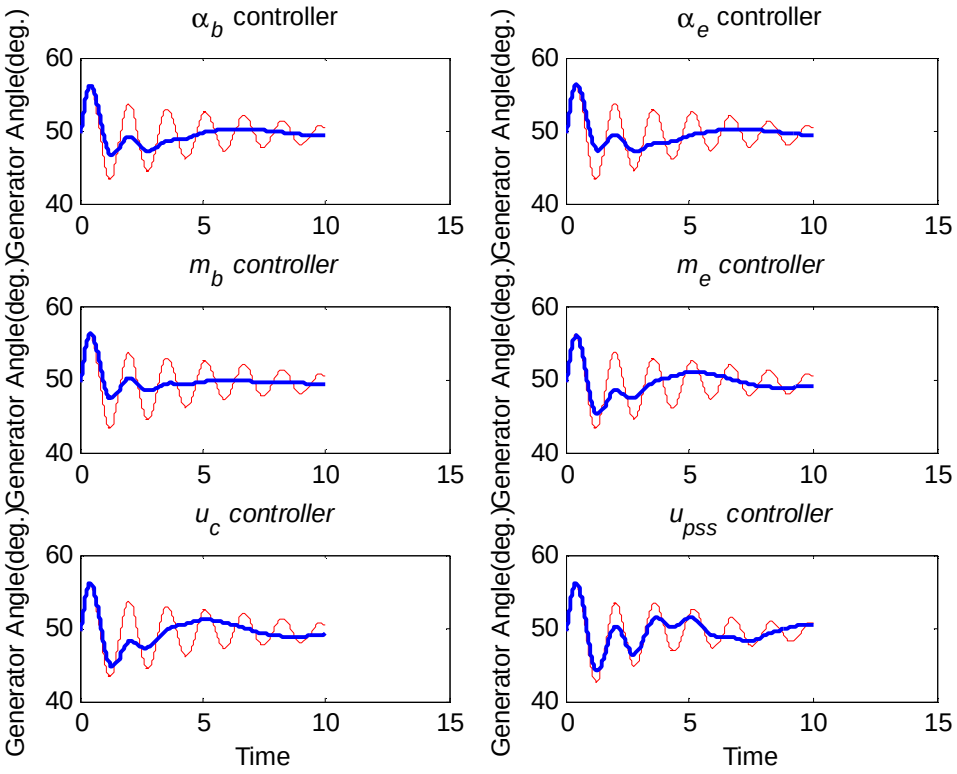

Figure 6.6: Generator rotor angle variation following a 10% torque pulse for 0.1 sec, with and without PI pole placement method

6.3 COMPARISON BETWEEN DAMPING CONTROLLERS

In the earlier sections, the hierarchy of damping control was established through decomposition methods, followed by simulation results on the power system considering the different controller structures. This section summarizes the results obtained by reorganizing the simulation results with the various damping controllers:

1- Lead-lag controller.

2- PI controller designed through residue principle.

3- PI controller design through pole placement method.

The responses with the six control inputs for all the three control design scenarios are presented in the following

6.3.1 LEAD-LAG CONTROLLER

Figures 6.7 and 6.8 show the performance of the four UPFC controls (m_e, a_e, m_b, a_b) when lead-lag method was used to design the controllers. Figure 6.7 shows the generator speed deviation while 6.8 shows the terminal voltage variation. For the ease of comparison, the same 10% input torque pulse case was compared.

Note, the response with the two other controls u_c and u_{pss} have not been included here to avoid congestion in the plots.

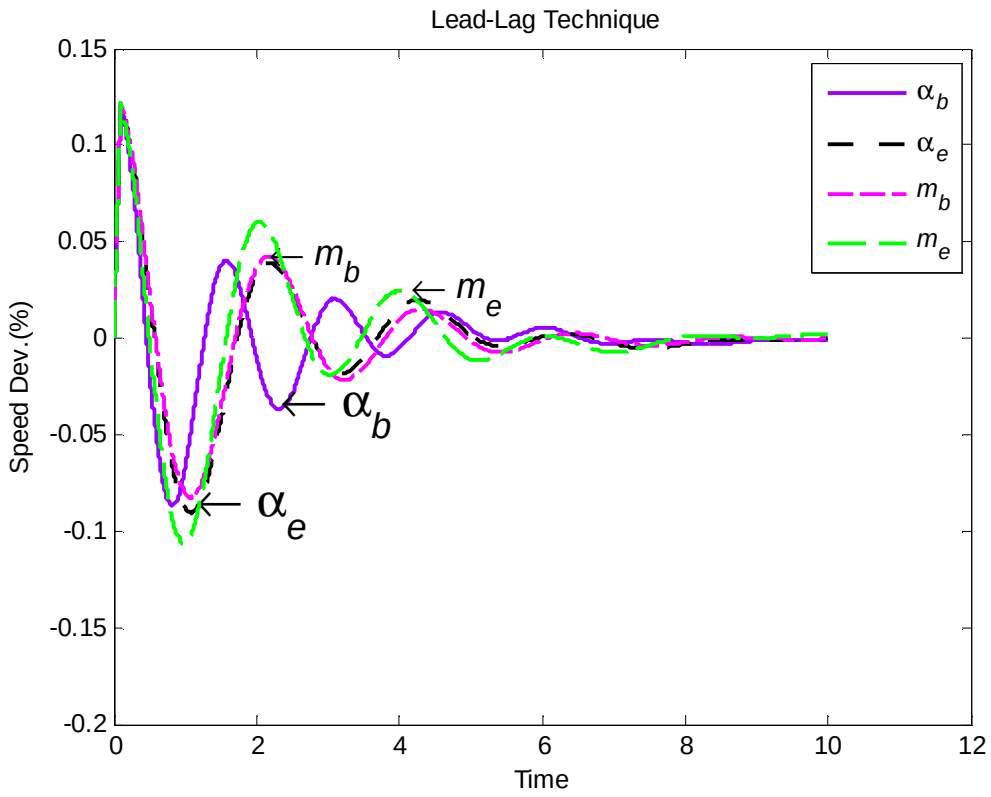

Figure 6.7: Generator speed variation with time following a 10% input torque pulse for 0.1 sec, with lead-lag controller

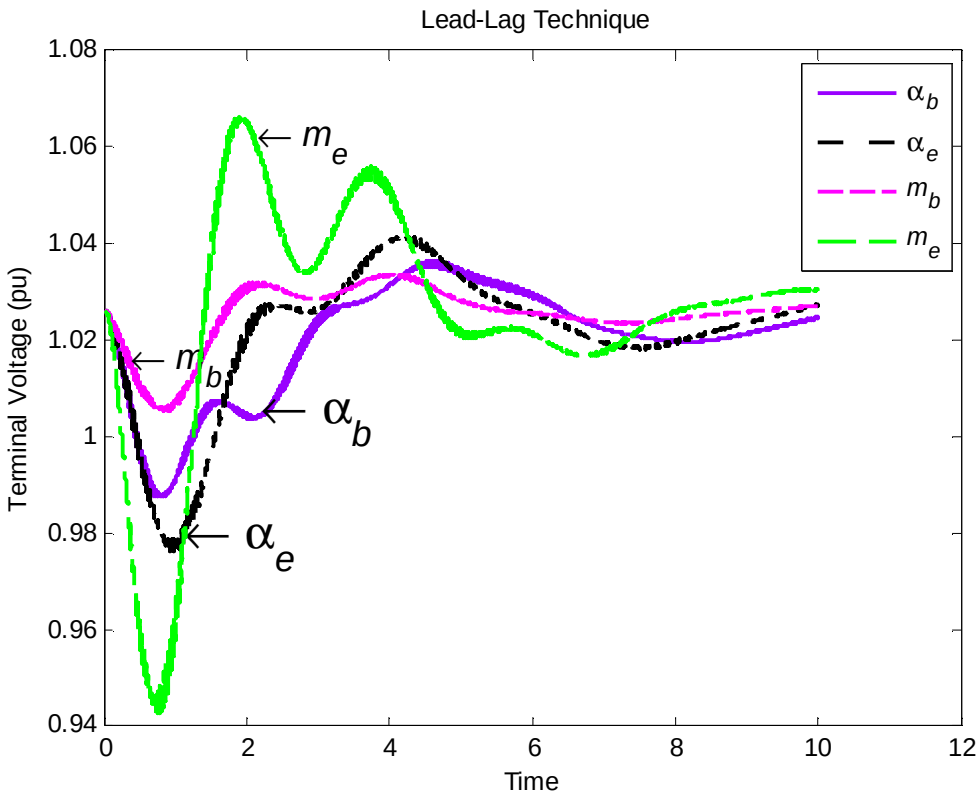

Figure 6.8: Terminal voltage variation with time following a 10% torque pulse for 0.1 sec, with lead-lag controller

Comparison of the responses presented in the two figures demonstrate that shunt converter phase angle provide the best damping compared with the others. The other inputs, in order damping profile are series converter voltage magnitude, series converter phase angle and shunt converter voltage magnitude, respectively.

6.3.2 PI CONTROLLER THROUGH RESIDUE METHOD

Figure 6.9 and 6.10 show the comparison of generator speed and terminal voltage responses with the UPFC controls when the *PI* controller derived through residue method

is used. Table 6.4 summarized the performance indices like peak overshoot, peak time, and settling time. A comparison of the indices are made considering a_e as the base case. The transient performance indices are extracted from the speed variation plot.

Observation of the transient responses in Figure 6.9 and 6.10 demonstrate that all the UPFC controls can be employed for stabilization through a *PI* controller. However, the best of them in terms of transient behavior is a_e. The maximum percent variation in terms of peak overshoot and settling times are a bout 0.6% and 13%, respectively.

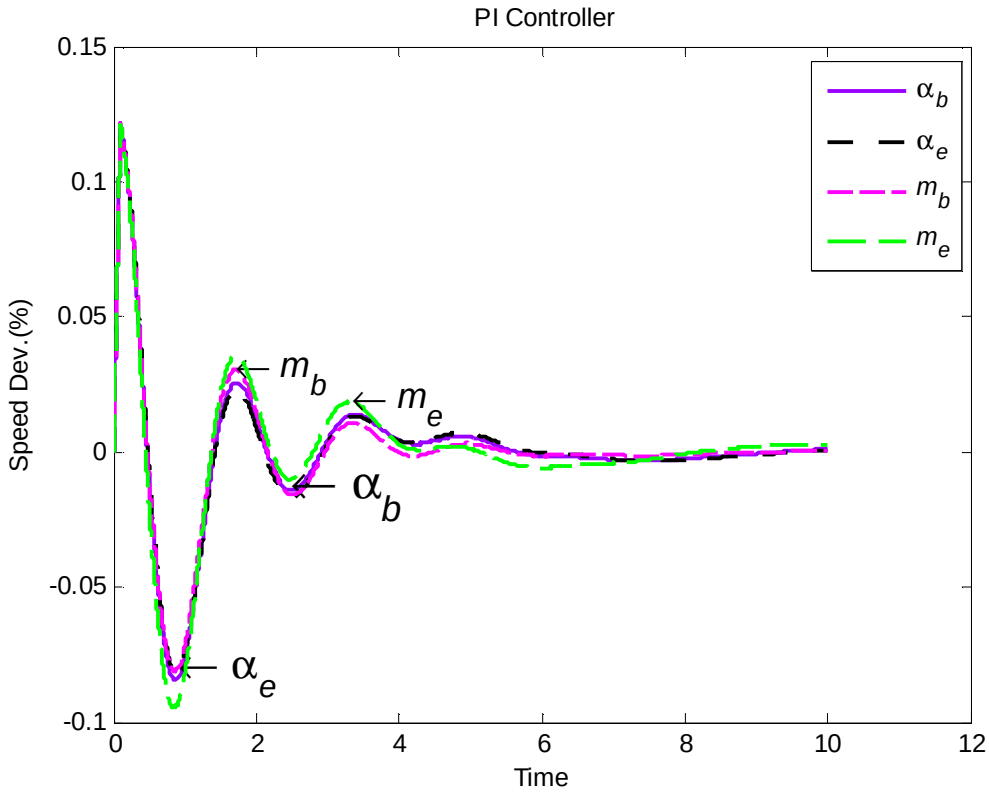

Figure 6.9: Generator speed variation with time following a 10% input torque pulse for 0.1 sec, with PI through residue method

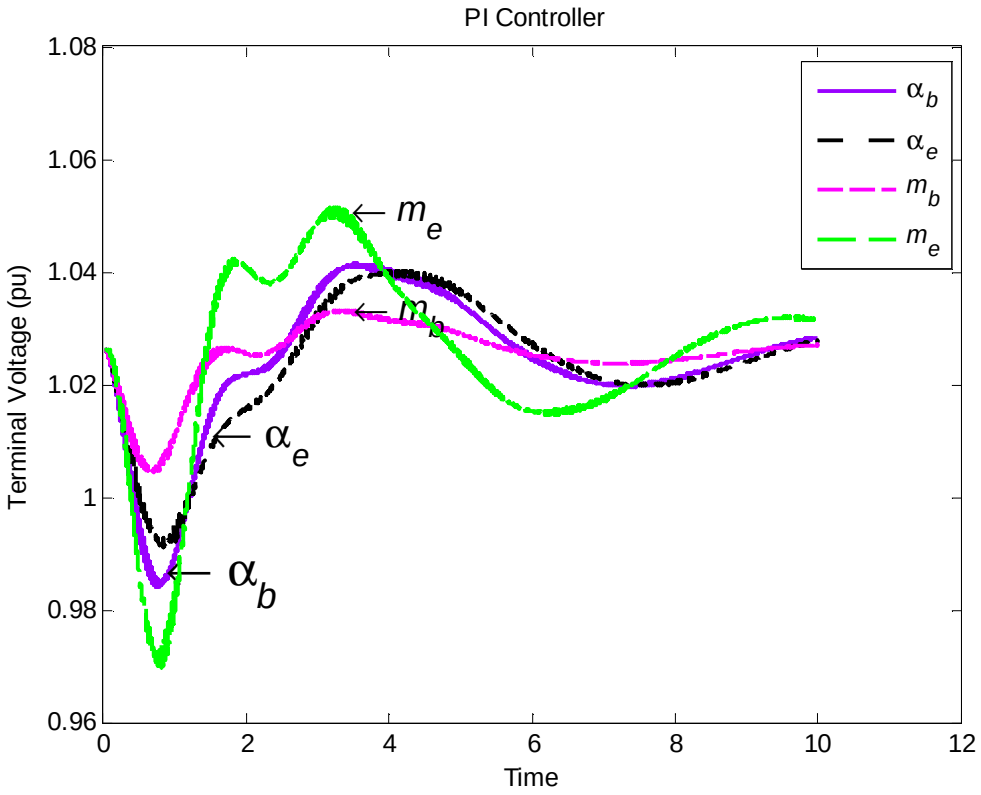

Figure 6.10: Terminal voltage variation with time following a 10% torque pulse for 0.1 sec, with PI through residue method

	Overshoot M_p (%)	Peak Time t_p (sec)	settling time, T_s (sec)	% Difference in M_p with a_e	% Difference in T_s with a_e
a_e	12.08	0.099	3.908	--------	-------
m_b	12.15	0.099	3.913	0.57947	0.127943
m_e	12.13	0.1	4.325	0.413907	10.67042
a_b	12.14	0.099	4.408	0.496689	12.79427

Table 6.4: Analysis of speed response for various performance indices

	Overshoot M_p (%)	Peak Time t_p (sec)	settling time, T_s (sec)	% Difference in M_p with a_e	% Difference in T_s with a_e
a_e	56.48	0.4844	5.228	--------	-------
m_b	56.54	0.4718	5.434	0.106232	3.940321
m_e	56.17	0.4428	5.962	-0.54887	14.03979
a_b	56.51	0.4756	5.987	0.053116	14.51798

Table 6.5: Analysis of angle response for various performance indices

6.3.3 PI POLE PLACEMENT TECHNIQUE

The *PI* design through the pole placement method forces the closed loop eignvalues to the desired location. Hence, it is expected that the transient response provided by this controller with the different inputs will be alike.

Figure 6.11 shows the transient speed variations following the pulse disturbance with the four UPFC controls. As, mentioned the transient responses are quite close, the best being provided by shunt converter phase angle (a_e), the other in order being series converter voltage magnitude (m_b), shunt converter voltage magnitude (m_e), and series converter

phase angle(a_b), respectively. The rotor angle signal in the integration of the speed signal, and hence the plot blows up the difference in response. Figure 6.12 demonstrates this.

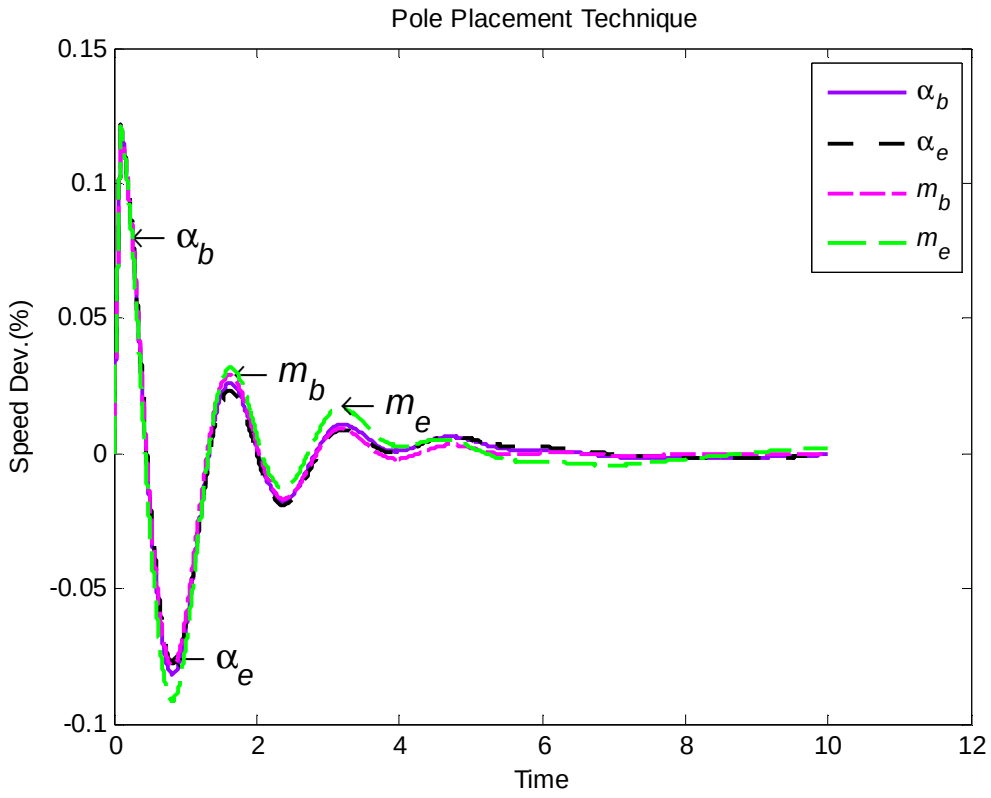

Figure 6.11: Generator speed variation with time following a 10% torque pulse for 0.1 sec, with PI through pole placement

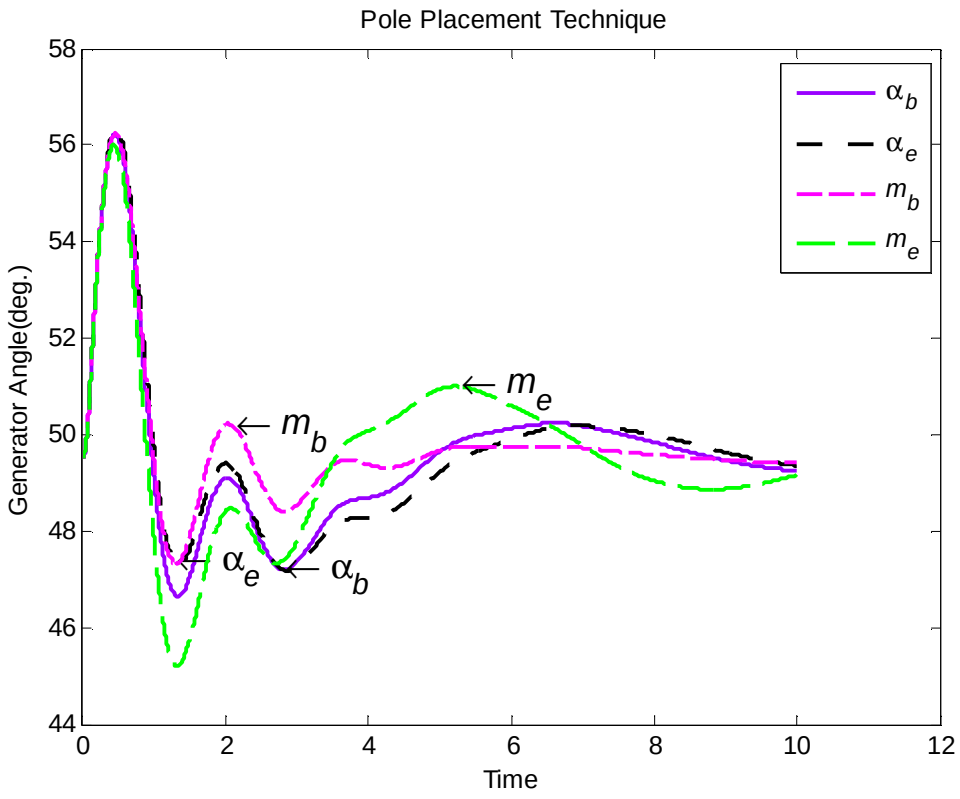

Figure 6.12: Generator rotor angle variation with time following a 10% torque pulse for 0.1 sec, with PI through pole placement

6.3.4 CAPACITOR AND POWER SYSTEM STABILIZER CONTROLS

Sections 6.3.1-6.3.3 compared the response of four UPFC controls. The other two controls, viz u_c and u_{pss} were not included for two reasons:

1- These two controls were not found to be as effective compared to the others.

2- To avoid the crowded responses on the same plot.

For the sake of completeness, the transient generator speed and angle responses with u_c, u_{pss} and a_e control (a_e was observed to be providing best damping) are compared

in Figures 6.13 and 6.14. As can be observed the transient response with a_e control is very superior to the other two.

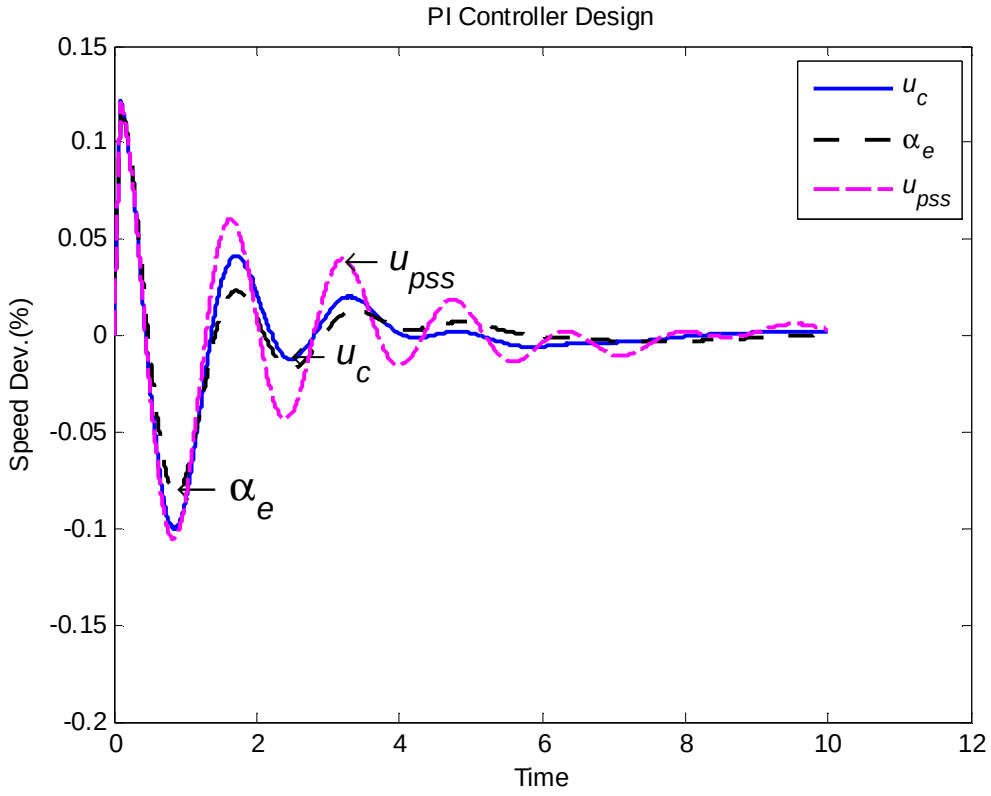

Figure 6.13: Generator speed variation with time following a 10% input torque pulse for 0.1 sec, with PI control through residue method for (a_e, u_c and u_{pss})

control

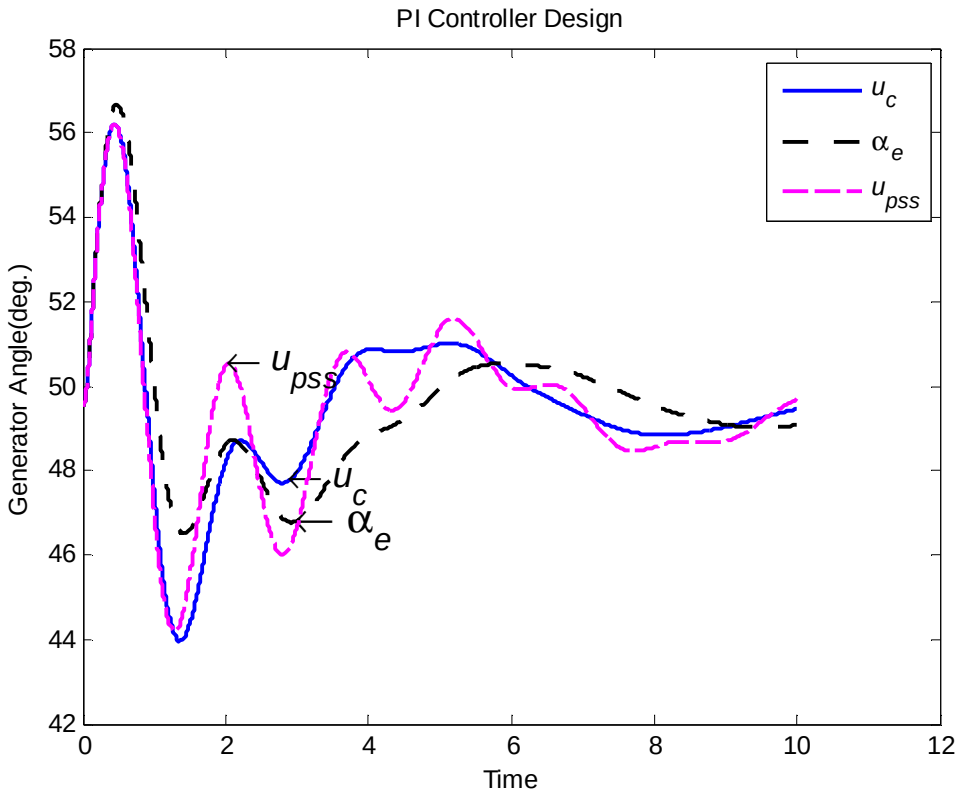

Figure 6.14: Generator rotor angle variation with time following a 10% input torque pulse for 0.1 sec, with PI control through residue method for (a_e, u_c and u_{pss}) controls

Table 6.6 gives a comparison of the performance indices with all the six controls designed with *PI* pole placement method. The best control signal a_e, in terms of damping enhancement, is compared with the remaining strategies. The maximum difference in terms of peak overshoot and settling time have been observed to be 0.7 % and 31%, respectively

	Overshoot M_p (%)	Peak Time t_p (sec)	settling time, T_s (sec)	% Difference in M_p with a_e	% Difference in T_s with a_e
a_e	12.08	0.099	3.908	--------	-------
m_b	12.15	0.099	3.913	0.57947	0.127943
m_e	12.13	0.1	4.325	0.413907	10.67042
a_b	12.14	0.099	4.408	0.496689	12.79427
u_c	12.17	0.1003	4.769	0.745033	22.03173
u_{pss}	12.13	0.099	5.116	0.413907	30.91095

Table 6.6: Analysis of speed response for various performance indices

6.4 SUMMERY OF THE CONTROL HIERARCHY ANALYSIS

The last three sections verify the hierarchy of the controls in terms of damping performance through simulation studies. Though the simulation results do not give precisely similar out comes, the general order of the six controls are

- Shunt converter phase angle (a_e)
- Series converter voltage magnitude (m_b)

- Power system stabilizer (u_{pss})
- Shunt converter voltage magnitude (m_e)
- Series converter phase angle (a_b)
- Capacitor control (u_c)

Note that the order established through simulation studies is compatible with the findings of the hierarchy study through various decomposition methods.

Figure 6.15 and 6.16 show a comparison of damping profiles with the three controller design techniques, lead-lag, PI through residue method and PI through pole placement method, for the most effective control identified (a_e). Figure 6.15 shows the speed variation and 6.16 the generator rotor angle for the pulse disturbance case.

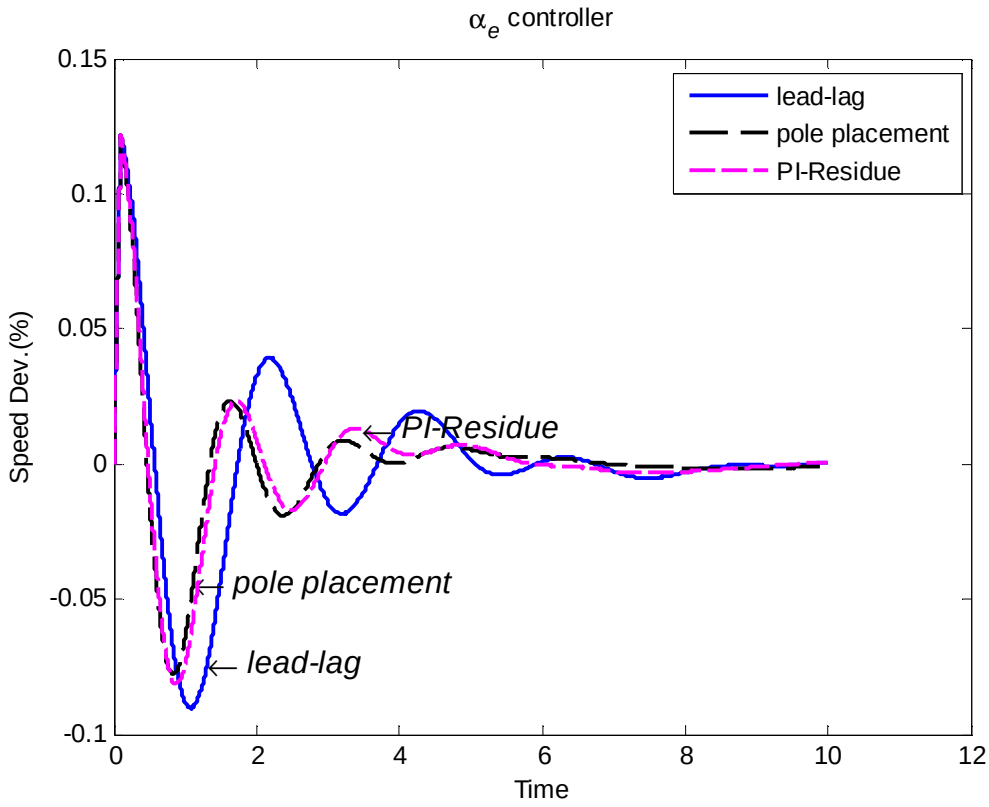

Figure 6.15: Generator speed variation with time following a 10% torque pulse for 0.1 sec, for a_e control

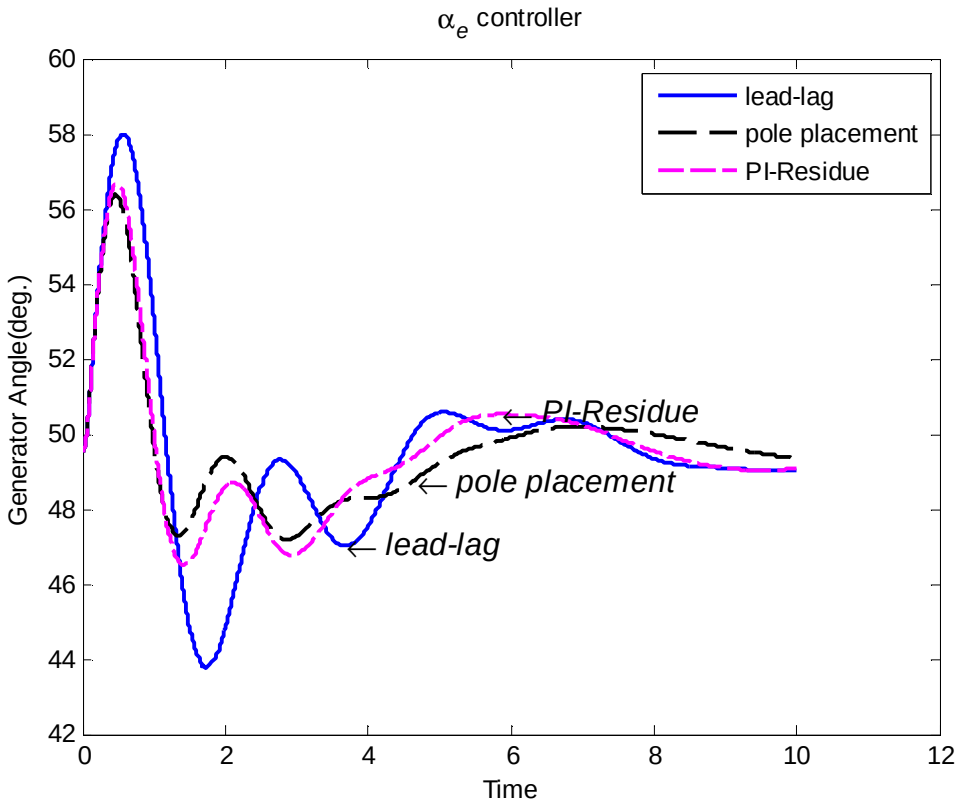

Figure 6.16: Generator rotor angle variation with time following a 10% torque pulse for 0.1 sec, for a_e control

6.5 SIMULATION STUDIES WITH SHUNT CONVERTER ANGLE

This section presents simulation studies on the SMIB system with UPFC for a number of disturbance conditions considering auxiliary control in the (a_e) input circuit. The *PI* controller using pole placement method has been used in this analysis because this was found to be the superior of the three controller designs in terms of damping improvement. Figure 6.17 show the non-linear synchronous generator speed response following a 10% input torque pulse with the proposed *PI* controller.

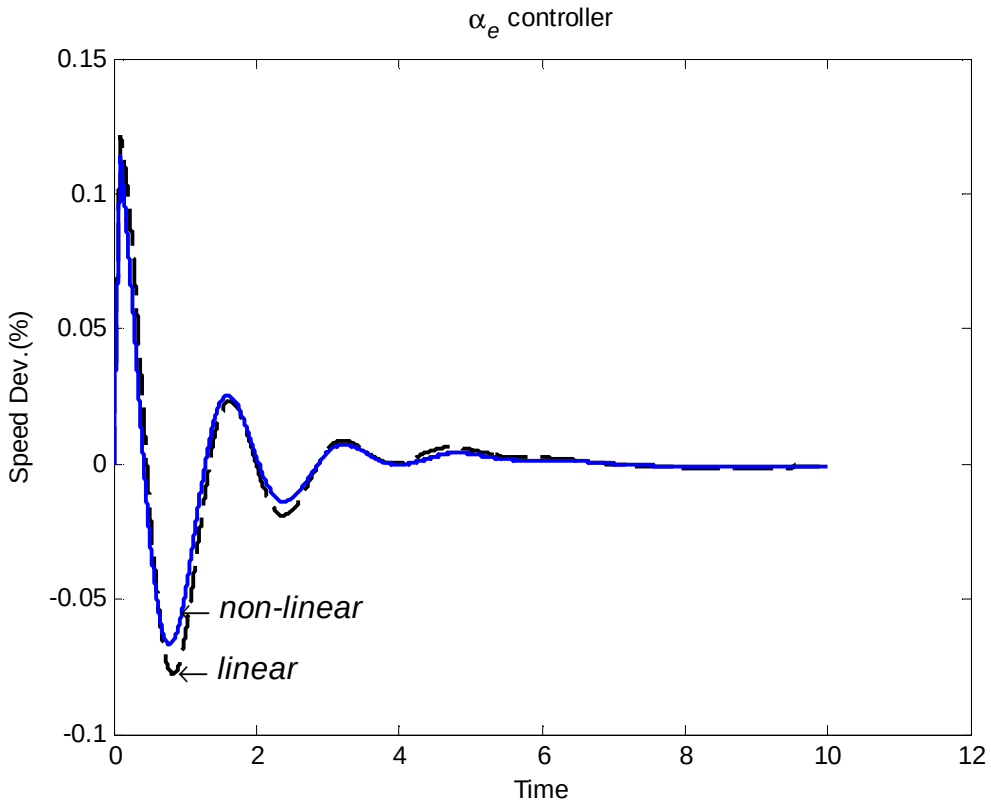

Figure 6.17: Generator speed variation with time following a 10% input torque pulse for 0.1 sec, linear and nonlinear response with PI controller

Figure 6.18 show the synchronous rotor angle response for different initial values, which is shown in Table 6.7, following a 10% input torque pulse with and without the proposed *PI* controller.

The response without control is oscillatory. While with controller seem to provide reasonable damping

Index	P_e	Q_e	V_t	d in degree	V_c
A	1.0127	0.3556	1.036	51.024	1.0127
B	0.8425	0.5525	1.0456	40.797	0.9869

C	1.3012	0.5439	1.0441	62.363	1.0108
D	0.6674	0.1254	1.0256	36.387	1.0217

Table 6.7: Initial values indices

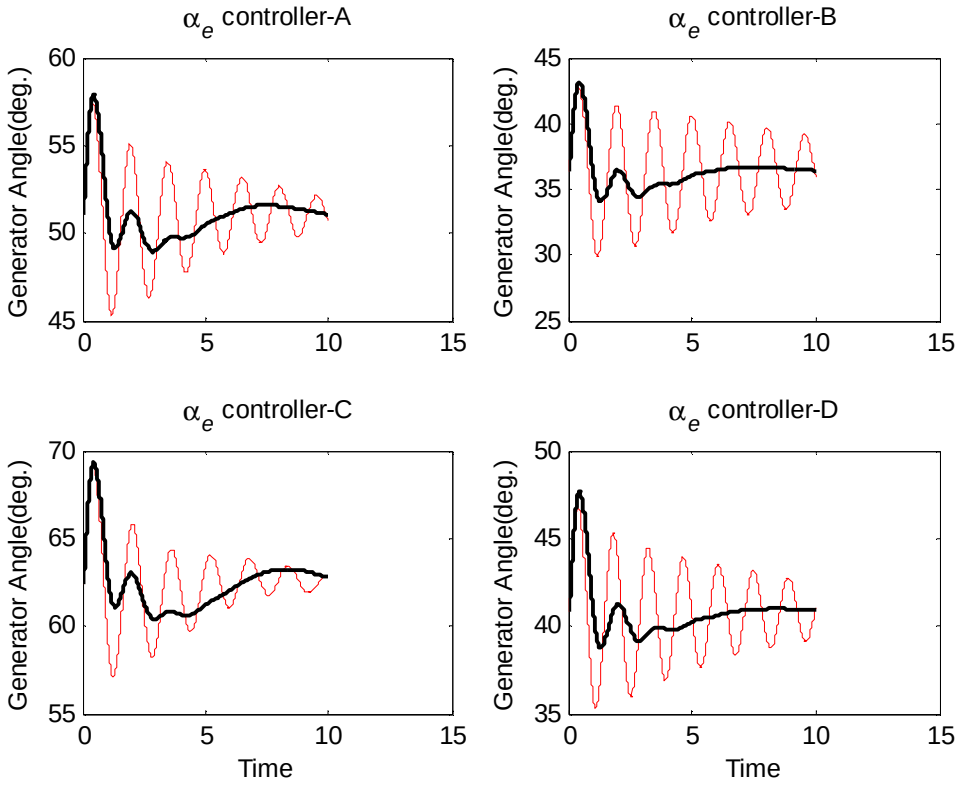

Figure 6.18: Generator rotor angle variation following a 10% torque pulse for 0.1 sec, with and without the PI controller

Figure 6.19 and 6.20 show the synchronous generator speed and terminal voltage response following a three-phase fault at infinite bus (V_b) for 0.2 second with the proposed *PI* controller. The control seems to provide reasonable damping.

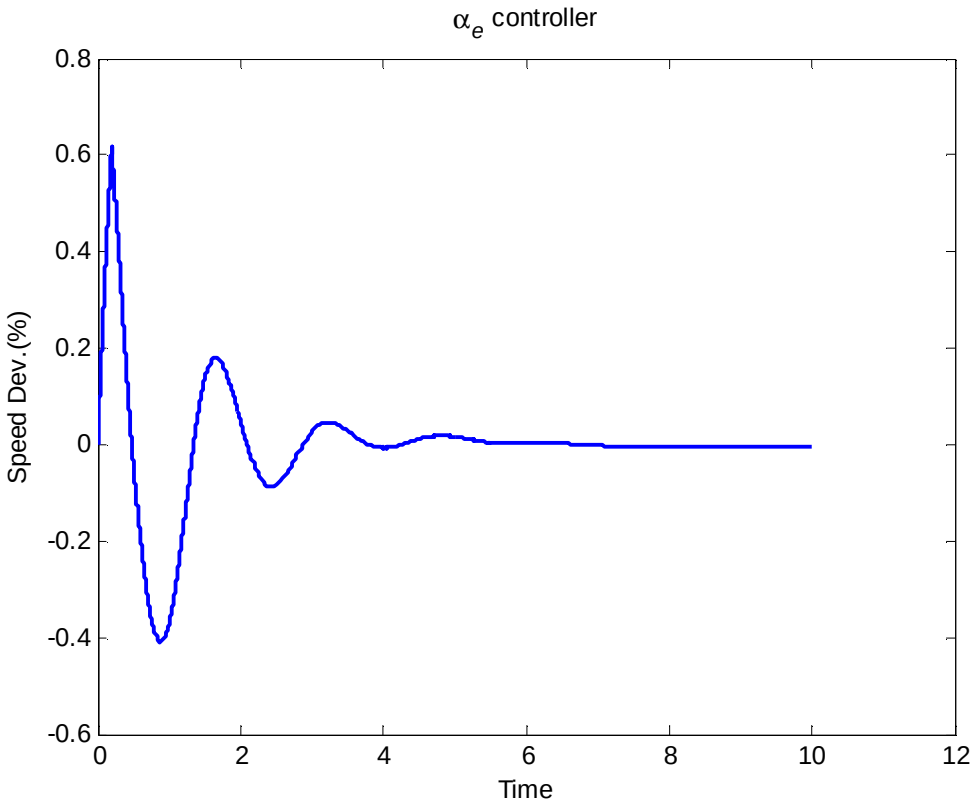

Figure 6.19: Generator speed variation with time following a three-phase fault for 0.2 sec, with the PI controller

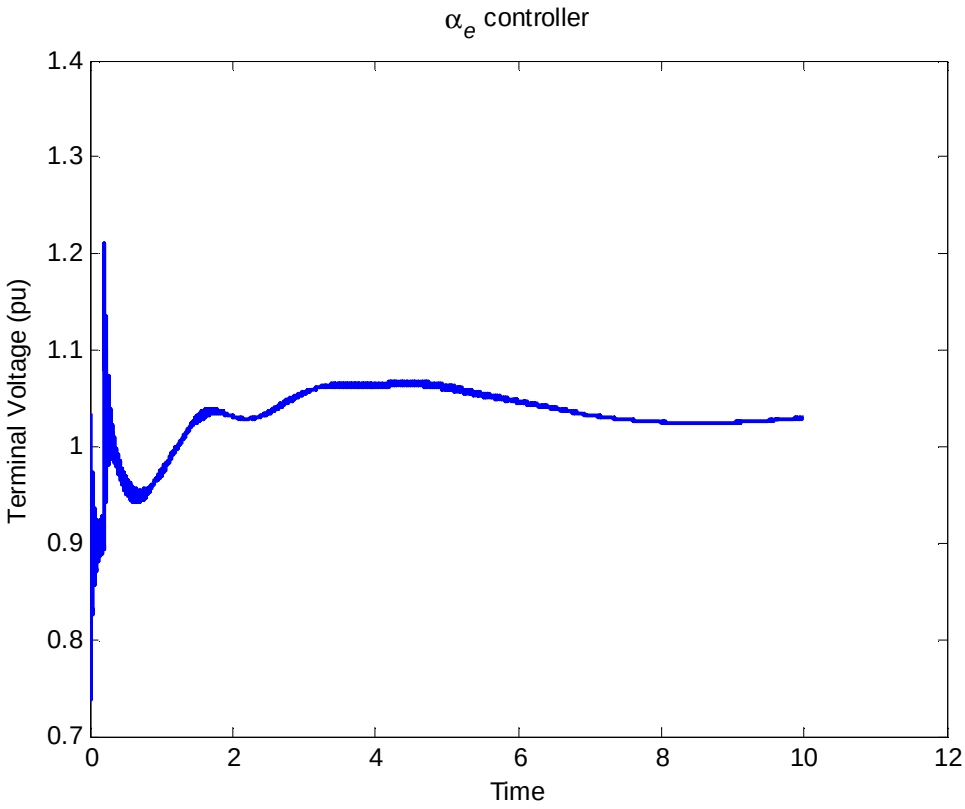

Figure 6.20: Terminal voltage variation with time following a three-phase fault for 0.2 sec, with the PI controller

CHAPTER 7

CONCLUSIONS & FUTURE WORK

7.1 CONCLUSIONS

The dynamic behavior of a single machine infinite bus (SMIB) system installed with UPFC has been investigated and the various controls which may be employed in damping power oscillations identified. The hierarchies of controls in terms of damping performance are established through singular value decomposition (SVD), residue method, and Hankel singular value (HSV). The various decomposition methods indicate that, shunt converter voltage phase angle (a_e) has the capability of providing best damping profile followed by series converter voltage magnitude(m_b), power system stabilizer (u_{pss}), shunt converter voltage magnitude (m_e), series converter phase angle

(a_b) and capacitor control (u_c) respectively. The singular value decomposition puts u_{pss} in the second places.

Three controller structures were examined to generate the additional stabilizing signals for the different control signals. All these three, the lead-lag compensator based *POD* design and two *PI* designs were observed to produce good additional stabilizing signals. Since *PI* design with pole placement method can directly effect the closed loop response, it was observed to provide better response.

The order of the stabilizing controls were verified by direct simulation of the system dynamics. It was observed, in general, that there was a good agreement of the findings of the simulation results with those found through decomposition techniques. PSS control though is widely used in power system studies, was only found to be at best in second place with respect to converter controls.

The designs of the controllers, were performed in the linear domain. Simulation studies with the nonlinear system model exhibited similar dynamic profile in terms of system damping.

The hierarchy study and control designs are relatively straight forward and has the potential of being applied to multi-machine power system.

7.2 FUTURE WORK

The following are the recommendations for future work:

- The controllers design techniques can be extended to two machines or multi-machine power system.
- The aspect of local and global control for multi-machine system can be explored.
- Machine speed has been considered to be the input signal to all the stabilizing circuits. Use of other input signals can be explored.

APPENDIX A

In this section we will linearize the non-linear equations for single machine infinite bus connected with UPFC as shown in Figure A1, the equations are as follows

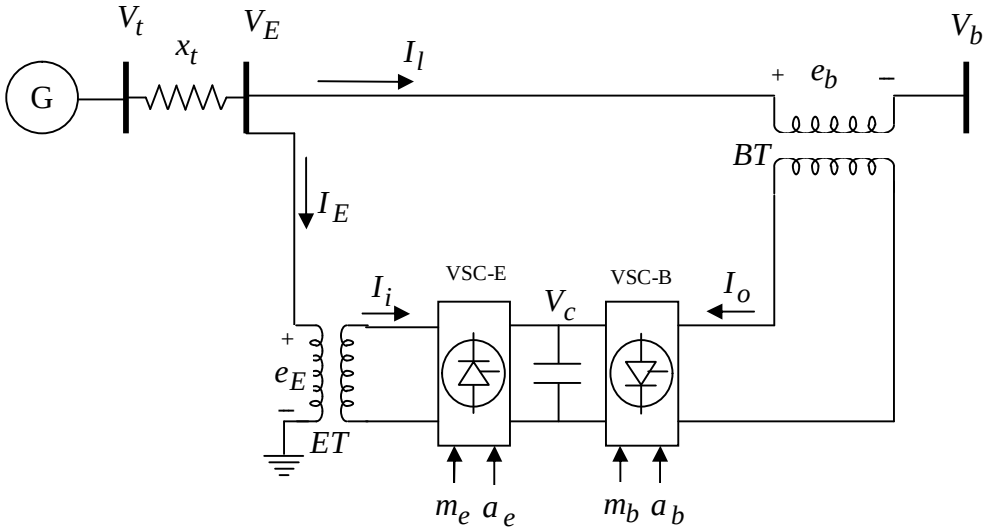

Figure A1: Power system with UPFC

$$\frac{dI_{ed}}{dt} = -w_o \frac{r_e}{L_e} I_{ed} + w_o(1+w) I_{eq} + \frac{w_o}{L_e}(v_{ed} - e_{ed})$$

$$\frac{dI_{eq}}{dt} = -w_o \frac{r_e}{L_e} I_{eq} - w_o(1+w) I_{ed} + \frac{w_o}{L_e}(v_{eq} - e_{eq})$$

$$\frac{dI_{ld}}{dt} = -w_o \frac{r_l}{L_l} I_{ld} + w_o(1+w) I_{lq} + \frac{w_o}{L_l}(v_{ed} - v_{bd} - e_{Bd})$$

$$\frac{dI_{lq}}{dt} = -w_o \frac{r_l}{L_l} I_{lq} - w_o(1+w) I_{ld} + \frac{w_o}{L_l}(v_{eq} - v_{bq} - e_{Bq})$$

$$\frac{dB}{dt} = -\frac{1}{T_c}[K_c \Delta v_c + B] + \frac{K_c}{T_c} u_c$$

$$\frac{dv_c}{dt} = \frac{1}{C + \frac{dB}{dt}}[m_e I_{ed} \cos a_e + m_e I_{eq} \sin a_e + m_b I_{ld} \cos a_b + m_b I_{lq} \sin a_b]$$

$$\frac{dd}{dt} = w_o w$$

$$\frac{dw}{dt} = \frac{1}{2H}[P_m - P_e - Dw]$$

$$\frac{de_q^{'}}{dt} = \frac{1}{T_{do}^{'}}[E_{fd} - e_{qo}^{'} - (x_d - x_d^{'}) I_d]$$

$$\frac{dE_{fd}}{dt} = \frac{K_r}{T_r}[v_{to} - v_t + u_{pss}] - \frac{E_{fd}}{T_r}$$

$$[1]\ \frac{dI_{ed}}{dt} = -w_o \frac{r_e}{L_e} I_{ed} + w_o(1+w) I_{eq} + \frac{w_o}{L_e}(v_{ed} - e_{ed})$$

$$sI_{ed} = -w_o \frac{r_e}{L_e} \Delta I_{ed} + w_o(1+w) \Delta I_{eq} + \frac{w_o}{L_e}(\Delta v_{ed} - \Delta e_{ed})$$

where

$$\Delta v_{ed} = (x_q + x_t)(\Delta I_{eq} + \Delta I_{lq})$$

$$\Delta e_{ed} = m_e \cos a_e \Delta V_c - m_e \sin a_e V_c \Delta a_e + \Delta m_e \cos a_e V_c$$

$$sI_{ed} = -w_o \frac{r_e}{L_e} \Delta I_{ed} + w_o(1+w) \Delta I_{eq} + \frac{w_o}{L_e}(x_q + x_t) \Delta I_{eq} + \frac{w_o}{L_e}(x_q + x_t) \Delta I_{lq}$$

$$- \frac{w_o}{L_e} m_e \cos(a_e) \Delta V_c + w_o I_{eq} \Delta w - \frac{w_o}{L_e} \Delta m_e \cos(a_e) V_c + \frac{w_o}{L_e} m_e \sin(a_e) V_c \Delta a_e$$

$$[2]\ \frac{dI_{eq}}{dt} = -w_o \frac{r_e}{L_e} I_{eq} - w_o(1+w) I_{ed} + \frac{w_o}{L_e}(v_{eq} - e_{eq})$$

$$sI_{eq} = -w_o \frac{r_e}{L_e} \Delta I_{eq} - w_o(1+w)\Delta I_{ed} - w_o I_{ed} \Delta w + \frac{w_o}{L_e}(\Delta v_{eq} - \Delta e_{eq})$$

where,

$$\Delta v_{eq} = \Delta e'_{eq} - (x'_d + x_t)(\Delta I_{ed} + \Delta I_{ld})$$

$$\Delta e_{eq} = m_e \sin a_e \Delta V_c + m_e \cos a_e V_c \Delta a_e + \Delta m_e \sin a_e V_c$$

$$sI_{eq} = [-w_o - \frac{w_o}{L_e}(x'_d + x_t)\Delta I_{ed} - w_o \frac{r_e}{L_e} \Delta I_{eq} - \frac{w_o}{L_e}(x'_d + x_t)\Delta I_{ld} - \frac{w_o}{L_e} m_e \cos(a_e)\Delta V_c$$

$$- w_o I_{ed} \Delta w + \frac{w_o}{L_e} \Delta e'_q - \frac{w_o}{L_e} V_c \sin(a_e)\Delta m_e - \frac{w_o}{L_e} m_e V_c \cos(a_e)\Delta a_e$$

$$[3]\ \frac{dI_{ld}}{dt} = -w_o \frac{r_l}{L_l} I_{ld} + w_o(1+w) I_{lq} + \frac{w_o}{L_l}(v_{ed} - v_{bd} - e_{Bd})$$

$$sI_{ld} = -w_o \frac{r_l}{L_i} \Delta I_{ld} + w_o(1+w) \Delta I_{lq} + \frac{w_o}{L_i}(\Delta v_{ed} - \Delta v_{bd} - \Delta e_{Bd})$$

where,

$$\Delta v_{ed} = (x_q + x_t)(\Delta I_{eq} + \Delta I_{lq})$$

$$\Delta v_{bd} = v_b \cos(d_{e_q} - d_{v_b}) \Delta d$$

$$\Delta e_{Bd} = m_b \cos a_b \Delta V_c - m_b \sin a_b V_c \Delta a_b + \Delta m_b \cos a_b V_c$$

$$sI_{ld} = -w_o \frac{r_l}{L_i} \Delta I_{ld} + w_o(1+w) \Delta I_{lq} + \frac{w_o}{L_i}((x_q + x_t)(\Delta I_{eq} + \Delta I_{lq})$$
$$- v_b \cos(d_{e_q} - d_{v_b}) \Delta d - m_b \cos a_b \Delta V_c - m_b \sin a_b V_c \Delta a_b + \Delta m_b \cos a_b V_c)$$

$$sI_{ld} = \frac{w_o}{L_i}(x_q + x_t) \Delta I_{eq} - w_o \frac{r_l}{L_i} \Delta I_{ld} + [w_o + \frac{w_o}{L_i}(x_q + x_t)] \Delta I_{lq} - \frac{w_o}{L_i} m_b \cos a_b \Delta V_c$$
$$- \frac{w_o}{L_i} v_b \cos(d) \Delta d + w_o I_{lq} \Delta w - \frac{w_o}{L_i} V_c \cos(a_b) \Delta m_b + \frac{w_o}{L_i} V_c m_b \sin(a_b) \Delta a_b$$

$$[4]\ \frac{dI_{lq}}{dt} = -w_o \frac{r_l}{L_l} I_{lq} - w_o(1+w) I_{ld} + \frac{w_o}{L_l}(v_{eq} - v_{bq} - e_{Bq})$$

$$sI_{lq} = -w_o \frac{r_l}{L_i} \Delta I_{lq} - w_o(1+w) \Delta I_{ld} + \frac{w_o}{L_i}(\Delta v_{eq} - \Delta v_{bq} - \Delta e_{Bq})$$

where,

$$\Delta v_{eq} = \Delta e'_{sq} - (x'_d + x_t)(\Delta I_{ed} + \Delta I_{ld})$$

$$\Delta v_{bq} = v_b \sin(d_{e_q} - d_{v_b}) \Delta d$$

$$\Delta e_{Bq} = m_b \sin a_b \Delta V_c + m_b \cos a_b V_c \Delta a_b + \Delta m_b \sin a_b V_c$$

$$sI_{lq} = -w_o \frac{r_l}{L_i} \Delta I_{lq} - w_o(1+w) \Delta I_{ld} + \frac{w_o}{L_i}(\Delta e'_{eq} - (x'_d + x_t)(\Delta I_{ed} + \Delta I_{ld})$$
$$- v_b \sin(d_{e_q} - d_{v_b}) \Delta d - m_b \sin a_b \Delta V_c - m_b \cos a_b V_c \Delta a_b - \Delta m_b \sin a_b V_c)$$

$$sI_{lq} = -\frac{w_o}{L_i}(x'_d + x_t) \Delta I_{ed} - [w_o(1+w) + \frac{w_o}{L_i}(x'_d + x_t)] \Delta I_{ld} - w_o \frac{r_l}{L_i} \Delta I_{lq}$$
$$- \frac{w_o}{L_i} m_b \sin a_b \Delta V_c - \frac{w_o}{L_i} v_b \sin(d) \Delta d - w_o I_{ld} \Delta w - \frac{w_o}{L_i} \Delta e'_q - \frac{w_o}{L_i} \sin(a_b) V_c \Delta m_b$$
$$- \frac{w_o}{L_i} m_b V_c \cos(a_b) \Delta a_b$$

[5] $$\frac{dB}{dt} = -\frac{1}{T_c}[K_c \Delta v_c + B] + \frac{K_c}{T_c} u_c$$

$$sB = -\frac{1}{T_c}[K_c \Delta v_c + \Delta B] + \frac{K_c}{T_c} \Delta u_c$$

$$sB = -\frac{K_c}{T_c} \Delta v_c - \frac{1}{T_c} \Delta B + \frac{K_c}{T_c} \Delta u_c$$

[6] $$\frac{dv_c}{dt} = \frac{1}{C + \frac{dB}{dt}}[m_e I_{ed} \cos a_e + m_e I_{eq} \sin a_e + m_b I_{ld} \cos a_b + m_b I_{lq} \sin a_b]$$

$$sV_c = (\frac{1}{c+B}) \times m_e \cos(a_e) \Delta I_{ed}$$
$$+ (\frac{1}{c+B}) \times m_e \sin(a_e) \Delta I_{eq}$$
$$+ (\frac{1}{c+B}) \times m_b \cos(a_b) \Delta I_{ld}$$
$$+ (\frac{1}{c+B}) \times m_b \sin(a_b) \Delta I_{lq}$$
$$- \frac{1}{T_c}[m_e(I_{ed} \cos(a_e) + I_{eq} \sin(a_e)) + m_b(I_{ld} \cos(a_b) - I_{lq} \sin(a_b))] \times \left(\frac{-1}{c+B}\right)^2 \Delta B$$
$$- \frac{K_c}{T_c}[m_e(I_{ed} \cos(a_e) + I_{eq} \sin(a_e)) + m_b(I_{ld} \cos(a_b) - I_{lq} \sin(a_b))] \times \left(\frac{-1}{c+B}\right)^2 \Delta V_c$$
$$+ \left(\frac{1}{c+B}\right)[I_{ed} \cos(a_e) + I_{eq} \sin(a_e)] \Delta m_e$$
$$- \left(\frac{1}{c+B}\right)[I_{ed} \sin(a_e) - I_{eq} \cos(a_e)] m_i \Delta a_e$$
$$+ \left(\frac{1}{c+B}\right)[I_{ld} \cos(a_b) + I_{lq} \sin(a_b)] \Delta m_b$$
$$- \left(\frac{1}{c+B}\right)[I_{ld} \sin(a_b) - I_{lq} \cos(a_b)] m_b \Delta a_b$$
$$+ \frac{K_c}{T_c}[m_e(I_{ed} \cos(a_e) + I_{eq} \sin(a_e)) + m_b(I_{ld} \cos(a_b) - I_{lq} \sin(a_b))] \times \left(\frac{-1}{c+B}\right)^2 \Delta u_c$$

[7] $$\frac{dd}{dt} = w_o w$$

$$s\,\Delta d = w_o \Delta w$$

[8] $$\frac{dw}{dt} = \frac{1}{2H}[P_m - P_e - Dw]$$

$$T_e = v_d I_d + v_q I_q$$

$$= x_q I_q I_d + (e_q^{'} - x_d^{'} I_d) \times I_d$$

$$= e_q^{'} I_q + (x_q - x_d^{'}) I_q I_d$$

$$= e_q^{'}(I_{eq} + I_{lq}) + (x_q - x_d^{'})(I_{eq} + I_{lq})(I_{ed} + I_{ld})$$

$$= e_q^{'}\Delta I_{eq} + e_q^{'}\Delta I_{lq} + (I_{eq} + I_{lq})\Delta e_q^{'} + (x_q - x_d^{'})(I_{ed} + I_{ld})\Delta I_{eq}$$

$$+ (x_q - x_d^{'})(I_{ed} + I_{ld})\Delta I_{lq} + (x_q - x_d^{'})(I_{eq} + I_{lq})\Delta I_{ed}$$

$$+ (x_q - x_d^{'})(I_{eq} + I_{lq})\Delta I_{ld}$$

$$sw = \frac{1}{2H}(-T_e - D\Delta w)$$

$$2 \times H \times (sw + D\Delta w) = -(x_q - x_d^{'})(I_{eq} + I_{lq})\Delta I_{ed} - [e_q^{'} + (x_q - x_d^{'})(I_{ed} + I_{ld})]\Delta I_{eq}$$

$$-(x_q - x_d^{'})(I_{eq} + I_{lq})\Delta I_{ld} - [e_q^{'} + (x_q - x_d^{'})(I_{ed} + I_{ld})]\Delta I_{lq} - (I_{eq} + I_{lq})\Delta e_q^{'}$$

$$sw = -\frac{1}{2H}(x_q - x_d^{'})(I_{eq} + I_{lq})\Delta I_{ed} - \frac{1}{2H}[e_q^{'} + (x_q - x_d^{'})(I_{ed} + I_{ld})]\Delta I_{eq}$$

$$-\frac{1}{2H}(x_q - x_d^{'})(I_{eq} + I_{lq})\Delta I_{ld} - \frac{1}{2H}[e_q^{'} + (x_q - x_d^{'})(I_{ed} + I_{ld})]\Delta I_{lq} - \frac{D}{2H}\Delta w$$

$$-\frac{1}{2H}(I_{eq} + I_{lq})\Delta e_q^{'}$$

[9] $$\frac{de_q^{'}}{dt} = \frac{1}{T_{do}^{'}}[E_{fd} - e_{qo}^{'} - (x_d - x_d^{'})I_d]$$

$$se_q^{'} = \frac{1}{T_{do}^{'}}[\Delta E_{fd} - \Delta e_{qo}^{'} - (x_d - x_d^{'})(\Delta I_{ed} + \Delta I_{ld})$$

$$(1 + sT_{do}^{'})\Delta e_q^{'} = \Delta E_{fd} - (x_d - x_d^{'})\Delta I_{ed} - (x_d - x_d^{'})\Delta I_{ld}$$

$$se_q^{'} = \frac{1}{T_{do}^{'}}(x_d - x_d^{'})\Delta I_{ed} - \frac{1}{T_{do}^{'}}(x_d - x_d^{'})\Delta I_{ld} - \frac{1}{T_{do}^{'}}\Delta e_q^{'} + \frac{1}{T_{do}^{'}}\Delta E_{fd}$$

[10] $$\frac{dE_{fd}}{dt} = \frac{K_r}{T_r}[v_{to} - v_t + u_{pss}] - \frac{E_{fd}}{T_r}$$

$$sE_{fd} = -\frac{K_r}{T_r}\Delta v_t + \frac{K_r}{T_r}\Delta u_{pss} - \frac{1}{T_r}\Delta E_{fd}$$

$$v_t^2 = v_d^2 + v_q^2$$

$$\Delta v_t = -\frac{v_{qo}}{v_{to}}x_d^{'}\Delta I_{ed} + \frac{v_{do}}{v_{to}}x_q\Delta I_{eq} - \frac{v_{qo}}{v_{to}}x_d^{'}\Delta I_{ld} + \frac{v_{do}}{v_{to}}x_q\Delta I_{lq} + \frac{v_{qo}}{v_{to}}\Delta e_q^{'}$$

$$sE_{fd} = \frac{K_r}{T_r}[\frac{v_{qo}}{v_{to}}x_d^{'}\Delta I_{ed} - \frac{v_{do}}{v_{to}}x_q\Delta I_{eq} + \frac{v_{qo}}{v_{to}}x_d^{'}\Delta I_{ld} - \frac{v_{do}}{v_{to}}x_q\Delta I_{lq} + \frac{v_{qo}}{v_{to}}\Delta e_q^{'}]$$

$$-\frac{1}{T_r}\Delta E_{fd} + \frac{K_r}{T_r}\Delta u_{pss}$$

$$sE_{fd} = (\frac{K_r}{T_r})\times(\frac{v_{qo}}{v_{to}})x_d^{'}\Delta I_{ed} - (\frac{K_r}{T_r})\times(\frac{v_{do}}{v_{to}})x_q\Delta I_{eq} + (\frac{K_r}{T_r})\times(\frac{v_{qo}}{v_{to}})x_d^{'}\Delta I_{ld}$$

$$-(\frac{K_r}{T_r})\times(\frac{v_{do}}{v_{to}})x_q\Delta I_{lq} + (\frac{K_r}{T_r})\times(\frac{v_{qo}}{v_{to}})\Delta e_q^{'} - \frac{1}{T_r}\Delta E_{fd} + \frac{K_r}{T_r}\Delta u_{pss}$$

APPENDIX B

$$kk = -\frac{1}{T_c}\left[m_e\left(I_{ed}\cos(a_e) + I_{eq}\sin(a_e)\right) + m_b\left(I_{ld}\cos(a_b) - I_{lq}\sin(a_b)\right)\right]$$

$$\begin{bmatrix} I_{ed} \\ I_{eq} \\ I_{ld} \\ I_{lq} \\ U \\ V_c \\ d \\ w \\ e_q^{'} \\ E_{fd} \end{bmatrix} = \begin{bmatrix} -\frac{w\times r_e}{L_e} & w+\frac{w(x_q+x_t)}{L_e} & 0 & \frac{w(x_q+x_t)}{L_e} & 0 & -\frac{w\times m_e\times\cos(a_e)}{L_e} & 0 \\ -w-\frac{w(x_d^{'}+x_t)}{L_e} & \frac{-w\times r_e}{L_e} & -\frac{w(x_d^{'}+x_t)}{L_e} & 0 & 0 & -\frac{w\times m_e\times\sin(a_e)}{L_e} & 0 \\ 0 & \frac{w(x_q+x_t)}{L_l} & -\frac{w\times r_l}{L_l} & w+\frac{w(x_q+x_t)}{L_l} & 0 & -\frac{w\times m_b\times\cos(a_b)}{L_l} & -\frac{w\times V_b\cos(d_o)}{L_i} \\ \frac{-w(x_d^{'}+x_t)}{L_l} & 0 & -w-\frac{w(x_d^{'}+x_t)}{L_l} & -\frac{w\times r_l}{L_l} & 0 & -\frac{w\times m_b\times\sin(a_b)}{L_l} & -\frac{w\times V_b\sin(d_o)}{L_i} \\ 0 & 0 & 0 & 0 & -\frac{1}{T_c} & -\frac{K_c}{T_c} & 0 \\ \frac{m_e\cos(a_e)}{C_{dc}+CB} & \frac{m_e\sin(a_e)}{C_{dc}+CB} & \frac{m_b\cos(a_b)}{C_{dc}+CB} & \frac{m_b\sin(a_b)}{C_{dc}+CB} & kk\times\left(\frac{-1}{C_{dc}+CB}\right)^2 & k_c\times kk\times\left(\frac{-1}{C_{dc}+CB}\right)^2 & \\ 0 & 0 & 0 & 0 & 0 & 0 & 0 \\ \frac{-(x_q-x_d^{'})\times(I_{eq}+I_{lq})}{2H} & \frac{-(e_{qo}^{'}+(x_q-x_d^{'})\times(I_{eq}+I_{lq}))}{2H} & \frac{-(x_q-x_d^{'})\times(I_{eq}+I_{lq})}{2H} & \frac{-(e_{qo}^{'}+(x_q-x_d^{'})\times(I_{eq}+I_{lq}))}{2H} & 0 & 0 & 0 \\ \frac{-(x_d-x_d^{'})}{T_{do}^{'}} & 0 & \frac{-(x_d-x_d^{'})}{T_{do}^{'}} & 0 & 0 & 0 & 0 \\ \frac{K_r}{T_r}\left(\frac{V_{qo}}{V_{to}}\right)\times x_d^{'} & -\frac{K_r}{T_r}\left(\frac{V_{do}}{V_{to}}\right)\times x_q & \frac{K_r}{T_r}\left(\frac{V_{qo}}{V_{to}}\right)\times x_d^{'} & -\frac{K_r}{T_r}\left(\frac{V_{do}}{V_{to}}\right)\times x_q & 0 & 0 & 0 \end{bmatrix}$$

$$
\begin{bmatrix}
w \times I_{eq} & 0 & 0 \\
-w \times I_{ed} & \frac{w}{L_e} & 0 \\
w \times I_{lq} & 0 & 0 \\
-w \times I_{ld} & \frac{w}{L_l} & 0 \\
0 & 0 & 0 \\
0 & 0 & 0 \\
w & 0 & 0 \\
-\frac{D}{2H} & -\frac{(I_{eq}+I_{lq})}{2H} & 0 \\
0 & -\frac{1}{T_{do}^{'}} & \frac{1}{T_{do}^{'}} \\
0 & -(\frac{K_r}{T_r}) \times (\frac{V_{qo}}{V_{to}}) & -\frac{1}{T_r}
\end{bmatrix}
\begin{bmatrix}
I_{ed} \\ I_{eq} \\ I_{ld} \\ I_{lq} \\ U \\ V_c \\ d \\ w \\ e_q^{'} \\ E_{fd}
\end{bmatrix}
$$

$$
+
\begin{bmatrix}
-\frac{w \times V_c \times \cos(a_e)}{L_s} & \frac{w \times m_e \times V_c \times \sin(a_e)}{L_s} & 0 & 0 & 0 & 0 \\
-\frac{w \times V_c \times \sin(a_e)}{L_s} & -\frac{w \times m_e \times V_c \times \cos(a_e)}{L_s} & 0 & 0 & 0 & 0 \\
0 & 0 & -\frac{w \times V_c \times \cos(a_b)}{L_i} & \frac{w \times m_b \times V_c \times \sin(a_b)}{L_l} & 0 & 0 \\
0 & 0 & -\frac{w \times V_c \times \sin(a_b)}{L_l} & -\frac{w \times m_b \times V_c \times \cos(a_b)}{L_l} & 0 & 0 \\
0 & 0 & 0 & 0 & \frac{K_c}{T_c} & 0 \\
\frac{\cos(a_e) \times I_{ed} + \sin(a_e) \times I_{eq}}{C_{dc}+CB} & \frac{m_e(-\sin(a_e) \times I_{ed} + \cos(a_e) \times I_{eq})}{C_{dc}+CB} & \frac{\cos(a_b) \times I_{ld} + \sin(a_b) \times I_{lq}}{C_{dc}+CB} & \frac{m_b(-\sin(a_b) \times I_{ld} + \cos(a_b) \times I_{lq})}{C_{dc}+CB} & -k_c \times kk \times (\frac{-1}{C_{dc}+CB})^2 & 0 \\
0 & 0 & 0 & 0 & 0 & 0 \\
0 & 0 & 0 & 0 & 0 & 0 \\
0 & 0 & 0 & 0 & 0 & 0 \\
0 & 0 & 0 & 0 & 0 & \frac{K_r}{T_r}
\end{bmatrix}
\begin{bmatrix}
m_e \\ a_e \\ m_b \\ a_b \\ u_c \\ u_{pss}
\end{bmatrix}
$$

APPENDIX C

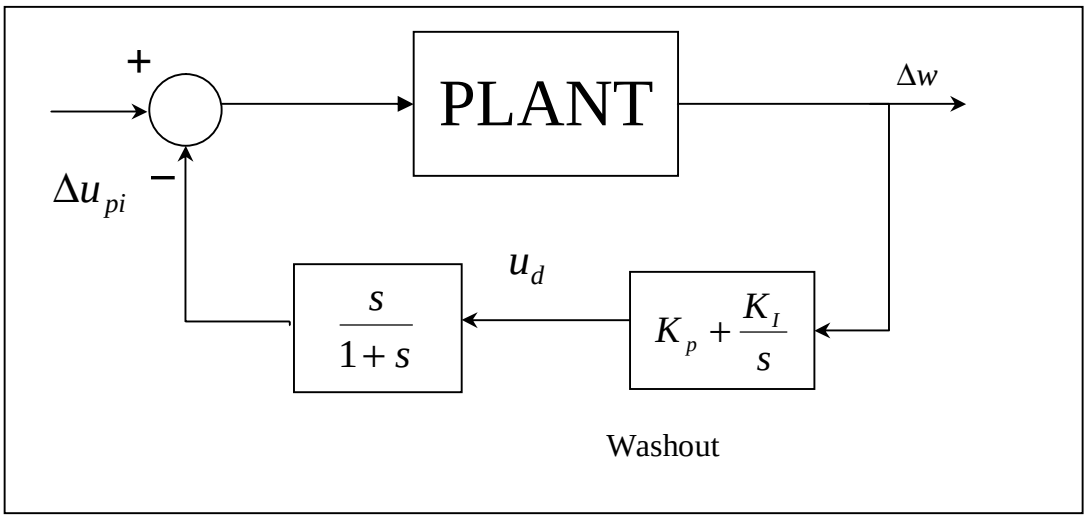

The derivation of the two new state equation of the PI through residue method

$$\frac{u_d}{\Delta w} = \frac{K_p s + K_I}{s}$$

$$\dot{u}_d = \Delta \dot{w} K_p + \Delta w K_I$$

$$\Rightarrow \quad \frac{du_d}{dt} = K_p\left(\frac{1}{2H}[P_m - P_e - D(w-1)]\right) + K_I \Delta w$$

$$\frac{u_{pi}}{u_d} = \frac{s}{1+s}$$

$$\dot{u}_{pi} = \dot{u}_d - u_{pi}$$

$$\Rightarrow \quad \frac{du_{pi}}{dt} = K_p\left(\frac{1}{2H}[P_m - P_e - D(w-1)]\right) + K_I \Delta w - \Delta u_{pi}$$

APPENDIX D

PI CONTROLLER

$$H(l) = \frac{1}{C(lI - A)^{-1}B} \quad \text{..... (1)}$$

or

$$H(l) = \frac{l}{1+l}\left(K_p + \frac{K_I}{l}\right) = \frac{lK_p}{1+l} + \frac{K_I}{1+l} \quad \text{..... (2)}$$

Substituting $l = s + jw$ into equ.(2), where λ is the desired eigenvalue of the closed-loop system equipped with the PI controller s is the real part of the desired eigenvalue and w is the imaginary part of the desired eigenvalue.

$$H(l) = \frac{(s + jw)}{1+(s + jw)}K_p + \frac{K_I}{1+(s + jw)}$$

Rearranging the above equation we get:

$$= \frac{(s + jw)}{(s +1) + jw}K_P + \frac{K_I}{(s +1) + jw}$$

Multiplying by the conjugate: $\frac{(1+s) - jw}{(1+s) - jw}$.

$$H(l) = \frac{(s + jw)[(s +1) - jw]}{(1+s)^2 + w^2}K_p + \frac{(s +1) - jw}{(s +1)^2 + w^2}K_I$$

$$= \frac{s(s+1)+w^2}{(s+1)^2+w^2}K_p + j\frac{w}{(s+1)^2+w^2}K_p + \frac{(s+1)}{(s+1)^2+w^2}K_I$$
$$- j\frac{w}{(s+1)^2+w^2}K_I$$

Collecting the real parts together and equating them with the real part of $H(l)$ in equ.(1)

$$\text{è}\ \frac{s(s+1)+w^2}{(s+1)^2+w^2}K_p + \frac{(s+1)}{(s+1)^2+w^2}K_I = real\ part\ of\ H(l) \ldots\ldots \text{(3)}$$

Similarly, collecting the imaginary parts together and equating them with the imaginary parts of $H(l)$.

$$\frac{w}{(s+1)^2+w^2}K_p - \frac{w}{(s+1)^2+w^2}K_I = imaginary\ part\ of\ H(l) \ldots\ldots \text{(4)}$$

APPENDIX E

$$kk = -\frac{1}{T_c}\left[m_e\left(I_{ed}\cos(a_i) + I_{eq}\sin(a_i)\right) + m_b\left(I_{ld}\cos(a_b) - I_{lq}\sin(a_b)\right)\right]$$

$$\begin{bmatrix} I_{ed} \\ I_{eq} \\ I_{ld} \\ I_{lq} \\ U \\ V_c \\ d \\ w \\ e_q^{'} \\ E_{fd} \\ u_d \\ u_{pi} \end{bmatrix} = \begin{bmatrix} -\frac{w\times r_e}{L_e} & w+\frac{w(x_q+x_t)}{L_e} & 0 & \frac{w(x_q+x_t)}{L_e} & 0 & -\frac{w\times m_e\times\cos(a_e)}{L_e} & 0 \\ -w-\frac{w(x_d^{'}+x_t)}{L_s} & \frac{-w\times r_e}{L_e} & -\frac{w(x_d^{'}+x_t)}{L_e} & 0 & 0 & -\frac{w\times m_e\times\sin(a_e)}{L_e} & 0 \\ 0 & \frac{w(x_q+x_t)}{L_l} & -\frac{w\times r_l}{L_l} & w+\frac{w(x_q+x_t)}{L_l} & 0 & -\frac{w\times m_b\times\cos(a_b)}{L_l} & -\frac{w\times V_b\cos(d_o)}{L_l} \\ \frac{-w(x_d^{'}+x_t)}{L_l} & 0 & -w-\frac{w(x_d^{'}+x_t)}{L_l} & -\frac{w\times r_l}{L_l} & 0 & -\frac{w\times m_b\times\sin(a_b)}{L_l} & -\frac{w\times V_b\sin(d_o)}{L_l} \\ 0 & 0 & 0 & 0 & -\frac{1}{T_c} & -\frac{K_c}{T_c} & 0 \\ \frac{m_e\cos(a_e)}{C_{dc}+CB} & \frac{m_e\sin(a_e)}{C_{dc}+CB} & \frac{m_b\cos(a_b)}{C_{dc}+CB} & \frac{m_b\sin(a_b)}{C_{dc}+CB} & kk\times\left(\frac{-1}{C_{dc}+CB}\right)^2 & k_c\times kk\times\left(\frac{-1}{C_{dc}+CB}\right)^2 & \\ 0 & 0 & 0 & 0 & 0 & 0 & 0 \\ \frac{-(x_q-x_d^{'})\times(I_{eq}+I_{lq})}{2H} & \frac{-(e_{qo}^{'}+(x_q-x_d^{'})\times(I_{eq}+I_{lq}))}{2H} & \frac{-(x_q-x_d^{'})\times(I_{eq}+I_{lq})}{2H} & \frac{-(e_{qo}^{'}+(x_q-x_d^{'})\times(I_{eq}+I_{lq}))}{2H} & 0 & 0 & 0 \\ \frac{-(x_d-x_d^{'})}{T_{do}^{'}} & 0 & \frac{-(x_d-x_d^{'})}{T_{do}^{'}} & 0 & 0 & 0 & 0 \\ \frac{K_r}{T_r}\left(\frac{V_{qo}}{V_{to}}\right)\times x_d^{'} & -\frac{K_r}{T_r}\left(\frac{V_{do}}{V_{to}}\right)\times x_q & \frac{K_r}{T_r}\left(\frac{V_{qo}}{V_{to}}\right)\times x_d^{'} & -\frac{K_r}{T_r}\left(\frac{V_{do}}{V_{to}}\right)\times x_q & 0 & 0 & 0 \\ -(x_q-x_d^{'})\times(I_{eq}+I_{lq})\times\left(\frac{K_p}{2H}\right) & \frac{-(e_{qo}^{'}+(x_q-x_d^{'})\times(I_{eq}+I_{lq}))\times K_p}{2H} & -(x_q-x_d^{'})\times(I_{eq}+I_{lq})\times\left(\frac{K_p}{2H}\right) & \frac{-(e_{qo}^{'}+(x_q-x_d^{'})\times(I_{eq}+I_{lq}))\times K_p}{2H} & 0 & 0 & 0 \\ -(x_q-x_d^{'})\times(I_{eq}+I_{lq})\times\left(\frac{K_p}{2H}\right) & \frac{-(e_{qo}^{'}+(x_q-x_d^{'})\times(I_{eq}+I_{lq}))\times K_p}{2H} & -(x_q-x_d^{'})\times(I_{eq}+I_{lq})\times\left(\frac{K_p}{2H}\right) & \frac{-(e_{qo}^{'}+(x_q-x_d^{'})\times(I_{eq}+I_{lq}))\times K_p}{2H} & 0 & 0 & 0 \end{bmatrix}$$

$$\begin{bmatrix} w\times I_{eq} & 0 & 0 & 0 & 0 \\ -w\times I_{ed} & \frac{w}{L_e} & 0 & 0 & 0 \\ w\times I_{lq} & 0 & 0 & 0 & 0 \\ -w\times I_{ld} & \frac{w}{L_l} & 0 & 0 & 0 \\ 0 & 0 & 0 & 0 & 0 \\ 0 & 0 & 0 & 0 & 0 \\ w & 0 & 0 & 0 & 0 \\ -\frac{D}{2H} & -\frac{(I_{eq}+I_{lq})}{2H} & 0 & 0 & 0 \\ 0 & -\frac{1}{T'_{do}} & \frac{1}{T'_{do}} & 0 & 0 \\ 0 & -(\frac{K_r}{T_r})\times(\frac{V_{qo}}{V_{to}}) & -\frac{1}{T_r} & 0 & 0 \\ k_i-(\frac{D\times K_p}{2H}) & -\frac{(I_{eq}+I_{lq})\times K_p}{2H} & 0 & 0 & 0 \\ k_i-(\frac{D\times K_p}{2H}) & -\frac{(I_{eq}+I_{lq})\times K_p}{2H} & 0 & 0 & -1 \end{bmatrix} \begin{bmatrix} I_{ed} \\ I_{eq} \\ I_{ld} \\ I_{lq} \\ U \\ V_c \\ d \\ w \\ e'_q \\ E_{fd} \\ u_d \\ u_{pi} \end{bmatrix}$$

$$+ \begin{bmatrix} -\frac{w\times V_c\times\cos(a_e)}{L_s} & \frac{w\times m_e\times V_c\times\sin(a_e)}{L_s} & 0 & 0 & 0 & 0 \\ -\frac{w\times V_c\times\sin(a_e)}{L_s} & -\frac{w\times m_e\times V_c\times\cos(a_e)}{L_s} & 0 & 0 & 0 & 0 \\ 0 & 0 & -\frac{w\times V_c\times\cos(a_b)}{L_l} & \frac{w\times m_b\times V_c\times\sin(a_b)}{L_i} & 0 & 0 \\ 0 & 0 & -\frac{w\times V_c\times\sin(a_b)}{L_l} & -\frac{w\times m_b\times V_c\times\cos(a_b)}{L_i} & 0 & 0 \\ 0 & 0 & 0 & 0 & \frac{K_c}{T_c} & 0 \\ \frac{\cos(a_e)\times I_{ed}+\sin(a_e)\times I_{eq}}{C_{dc}+CB} & \frac{m_e(-\sin(a_e)\times I_{ed}+\cos(a_e)\times I_{eq})}{C_{dc}+CB} & \frac{\cos(a_b)\times I_{ld}+\sin(a_b)\times I_{lq}}{C_{dc}+CB} & \frac{m_b(-\sin(a_b)\times I_{ld}+\cos(a_b)\times I_{lq})}{C_{dc}+CB} & -k_c\times kk\times(\frac{-1}{C_{dc}+CB})^2 & 0 \\ 0 & 0 & 0 & 0 & 0 & 0 \\ 0 & 0 & 0 & 0 & 0 & 0 \\ 0 & 0 & 0 & 0 & 0 & 0 \\ 0 & 0 & 0 & 0 & 0 & \frac{K_r}{T_r} \\ 0 & 0 & 0 & 0 & 0 & 0 \\ 0 & 0 & 0 & 0 & 0 & 0 \end{bmatrix} \begin{bmatrix} m_e \\ a_e \\ m_b \\ a_b \\ u_c \\ u_{pss} \end{bmatrix}$$

APPENDIX F

SINGLE MACHINE INFINITE BUS SYSTEM DATA

The parameters of the synchronous generator-UPFC system (per unit)

H=4s	x_d =1	$x_d^{'} = 0.3$	$x_q = 0.6$
K_r =6	$T_r = 0.05$	$T_{do}^{'} = 5.044$	w =377
D=0	T_c =0.05	K_c =50	

Line, Transformer resistance and Reactance

r_l =0	l_l =0.3	C_{dc} =3	x_t =0.05
x_e =0.1	L_e =0.1	r_e =0.01	r_b =0.01
x_b =0.1			

Selected operating quantities and other corresponding values:

V_e =1.02$\angle 0^o$	V_b =1$\angle -23^o$	P_e =0.93	Q_e =0.1488
$e_{qo}^{'}$ =1.0804	V_t =1.026	d =49.056°	m_e =1
m_b =0.1	E_{fd} =1.4487	V_c =1.0288	e_b =0.0926
a_b =2.3328°	e_e =1.0288	a_e =1.0716°	

REFERENCES

[1] G.W.Stagg and A.H.EL-abaid, “Computer methods in power systems (New york hills, 1968).

[2] P.K. Padiyar,“ Power system stability and control” EPRI Power system series 1994.

[3] P.M. Anderson and A.A.Fouad, “Power system control and stability”, Iowa state university press, 1980.

[4] Kimbark, “ Power system stability” , vol. 1

[5] Y.N. YU, “Electric power system dynamics”, Academic press 1983.

[6] E.Lerch, D.Porh and L.XU, “Advanced SVC control for damping power system oscillations”, 1991.

[7] N.Mithulananthan, C.A Canizares, J.Reeve and G.J.Rogers, “Comparison of PSS, SVC and STATCOM controllers for damping power system oscillations”. IEEE transactions on power systems, vol. 18, no.2, pp 786-792, May 2003.

[8] A.M.Stankovic, P.C.Stefanov, G.Tadnor and D.J.Somajic, “Dissipativity as a unifying control design framework for suppression of low frequency oscillations in power systems”. IEEE transaction on power system vol.14, no.1, pp 192-199 February 1999.

[9] J.Chen, J.V.Milanovic, and F.M.Huges, "Selection of auxiliary input signal and location of SVC for damping electro-mechanical oscillations". IEEE transactions on power system vol. pp 623-627 2001.

[10] D.N.Koterev, C.W.Taylor and W.A.Mittlestadt, "Model validation for August 10, 1996 WSCC system outage". IEEE transactions on power systems vol. 14, pp 967-979, August 1999.

[11] N. Mithlananthan and S.C.Srivastva, "Investigation of voltage collapse in srilanka's power system network". In proc EMPD Singapore, pp 47-52, March 1995, IEEE catalog 98 EX 137.

[12] Demello, P.J.Molan, T.F.Laskowski, and J. Udrill, "Co-ordinated application of stabilizers in multi-machine systems". IEEE transaction on PAS, vol. PAS -99, pp 892-902, 1980.

[13] Demello and C.Concordia, "Concepts of synchronous machine stability as affected by Excitation control". IEEE trans power APP and systems, vol. PAS 103, no 8, pp 1983-1989, 1984.

[14] Hingorani, N.G., "Flexible AC Transmission", *IEEE Spectrum*, April 1993, p. 40-44

[15] Gyugyi, L., "Dynamic Compensation of AC Transmission Lines by Solid-state Synchronous Voltage Sources", IEEE, 1993, p. 904-911

[16] Higorani, N.G, and Gyugyi,L.,"Understanding FACTS Devices", IEEE Press 2000

[17] Abu H.M.A. Rahim, Jamil M. Bakhashwain, and Samir A. Al-Baiyat, " A Robust Damping Controller Design for a Unified Power Flow Controller ", IEEE, Sept. 2004 p. 265 - 269 Vol. 1

[18] N.G.Hingoroni, "Flexible AC transmission system". Fifth IEE international conference on AC and DC transmission (IEE-pub. no 345), pp 1-7 September 1991.

[19] N.G.Hingoroni, "Flexible AC transmission systems", IEEE spectrum (40-45) April 1993.

[20] N.G.Hingoroni, "FACTS technology and opportunities IEEE colloquim". (Digest no. 1994/OCS) "FACTS the key to increased utilization of power system", pp 4/1- 4/10, Jan 1994.

[21] M.F.Kandlawala, "Investigation of dynamic behavior of power system installed with STATCOM", A thesis submitted to university of King Fahd University of Petroleum and Minerals, December 2001.

[22] Laszlo Gyugi, "converter based facts controller", IEE colloquium on FACTS pages 1-11, November 23, 1998.

[23] M.F.Kandlawala and A.H.M.A.Rahim, "Power system dynamic performance with

STATCOM controller". 8th annual IEEE technical exchange meeting, April 2001.

[24] L.O.Mak, Y.X.Ni and C.M.Shen, "STATCOM with fuzzy controller for interconnected power systems", Electric power system research, August 1999, pp 87-95.

[25] Y. H. Song, and A. T. Johns. "Flexible AC Transmission Systems (FACTS)", IEE Press, London, 1999. ISBN 0-85296-771-3.

[26] Y. Guo, D.J. Hill, and Y. Wang. "Global transient stability and voltage regulation for power systems", *IEEE Transactions on Power Systems*. VOL. 16, NO. 4. November 2001.

[27] J.Y. Liu; Y.H. Song; and P.A. Mehta, "Strategies for handling UPFC constraints in steady-state power flow and voltage control". *IEEE Transactions on Power Systems*. VOL. 15, May 2000, pp. 566–571.

[28] S. Gerbex, R. Cherkaoui, and A. J. Germond, "Optimal location of multi-type FACTS devices in a power system by means of genetic algorithms," *IEEE Trans. Power Systems*, vol. 16, August. 2001, pp. 537-544.

[29] Nabavi-Niaki, and Iravani, M.R., "Steady-state and Dynamic Models of Unified Power Flow Controller (UPFC) for Power System Studies", *IEEE Transactions of Power Systems*, Vol. 11, No. 4, November 1996, p. 1937-1943

[30] Wang, H.F., "Applications of Modelling UPFC into Multi-machine Power Systems", *IEE Proceedings Generation Transmission Distribution*, Vol. 146, No. 3, May 1999, p. 306-312

[31] Uzunovic, E., Canizares, C.A., and Reeve, J., "Fundamental Frequency Model of Unified Power Flow Controller", *North American Power Symposium*, NAPS, Cleveland, Ohio, October 1998

[32] Huang, Z., Ni, Y., Shen, C.M., Wu, F.F., Chen, S., and Zhang, B., "Application of Unified Power Flow Controller in Interconnected Power Systems -- Modeling, Interface, Control Strategy and Case Study", *IEEE Power Engineering Society Summer Meeting*, 1999

[33] Noroozian, M., Angquist, L., Ghandhari, M., and Andersson, G., "Use of UPFC for Optimal Power Flow Control", *IEEE Transactions on Power Delivery*, Vol. 12, No. 4, October 1997, p. 1629-1634

[34] P. Kundur, "Power System Stability and Control", EPRI, McGraw-Hill, 1994, ISBN 0-07-035958-X.

[35] G. Rogers, "Power System Oscillations", Kluwer Academic Publishers, December 1999.

[36] M.M. Farsangi, and Y.H. Song, "Choice of FACTS Device Control Inputs for Damping Interarea Oscillations", IEEE, Vol,19, No. 2, May 2004

[37] M. E. Aboul-Ela, A. A. Salam, J. D. McCalley and A. A. Fouad, "Damping controller design for power system oscillations using global signals", IEEE Transactions on Power System, Vol 11, No. 2, May 1996, pp 767-773

[38] N. Tambey and M. L. Kothari, "Unified Power Flow Controller (UPFC) Based Damping Controllers for Damping Low Frequency Oscillations in a Power System", Vol 84, June 2003

[39] Mohammed Dahleh, Munther A. Dahleh and George Verghese, Lectures on "Dynamic Systems and Control". Electrical Engineering ad Computer Science, Fall 2003.

[40] Ali Al-Awami, Y.L. Abdel-Magid, and M. A. Abido, "Simultaneous Stabilization of Power System Equipped with Unified Power Flow Controller Using Particle Swarm", 15th PSCC, Liege, 22-26 August 2005

[41] D. J. Trudnowski, "Order Reduction of Large Scale Linear Oscillatory System Models", IEEE Winter Power Meeting, February 1993

[42] Rusejla Sadikovic, Petr Korba and Goran Andersson, "Application of FACTS Devices for Damping of Power System Oscillations". IEEE Conference Proceddings, 27-30 June 2005

[43] Nabavi-Niaki, A., and Iravani, M.R., "Steady-state and Dynamic Models of Unified Power Flow Controller (UPFC) for Power System Studies", *IEEE Transactions of Power Systems*, Vol. 11, No. 4, November 1996, p. 1937-1943

[44] Fuerte-Esquivel, C.R., and Acha, E., "Unified Power Flow Controller: A Critical Comparision of Newton-Raphson UPFC algorithms in Power Flow Studies", *IEE Proceedings Generation Transmission Distribution*, Vol. 144, No. 5, September 1997, p. 437-444

[45] Fuerte-Esquivel, C.R., and Acha, E., "Newton-Raphson Algorithm for reliable Solution of Large Power Networks with Embedded FACTS Devices", *IEE Proceedings Generation Transmission Distribution*, Vol. 143, No. 5, September 1996, p. 447- 454

[46] Ambriz-Perez, H., Acha, E., and Fuerte-Esquivel, C.R, De la Torre, A., "Incorporation of a UPFC Model in an Optimal Power Flow Using Newton's Method", *IEE Proceedings Generation Transmission Distribution*, Vol. 145, No. 3, May 1998, p. 336-344

[47] Schauder, C., and Metha, H., "Vector Analysis and Control of Advanced Static VAR Compensators", *IEE Proceedings-C*, Vol. 140, No. 4, July 1993, p. 299-306

[48] Papic, I., Zunko, P., Povh, D., and Weinhold, M., "Basic Control of Unified Power Flow Controller", *IEEE Transactions of Power Systems*, Vol. 12, No. 4, November 1997, p. 1734-1739

[49] Smith, K.S., Ran, L., and Penman, J., "Dynamic Modeling of a Unified Power Flow Controller", *IEE Proceedings Generation Transmission Distribution*, Vol. 144, No. 1, January 1997, p. 7-12

[50] Padiyar, K.R., and Kulkarni, A.M., "Control Design and Simulation of Unified Power Flow Controller", *IEEE Transactions on Power Delivery*, Vol. 13, No. 4, October 1997, p. 1348-1354

[51] Wang, H.F., "Damping Function of Unified Power Flow Controller", *IEE Proceedings Generation Transmission Distribution*, Vol. 146, No. 1, January 1999, p. 81-87

[52] Wang, H.F., "Applications of Modelling UPFC into Multi-machine Power Systems", *IEE Proceedings Generation Transmission Distribution*, Vol. 146, No. 3, May 1999, p. 306-312

[53] Uzunovic, E., Canizares, C.A., and Reeve, J., "Fundamental Frequency Model of Unified Power Flow Controller", *North American Power Symposium*, NAPS, Cleveland, Ohio, October 1998

[54] Uzunovic, E., Canizares, C.A., and Reeve, J., "EMTP Studies of UPFC Power Oscillation Damping", *Proceedings of the North American Power Symposium (NAPS)*, San Luis Obispo, CA, October 1999, pp. 405-410

[55] Seo,J., Moon, S., Park, J. and Choe, J., "Design of a Robust UPFC Controller for Enhancing the Small Signal Stability in the Multi-machine Power Systems". IEEE Power Engineering Society Winter Meeting, 2001, Vol.3, pp. 1197-1202.

[56] S. Tara Kalyani, and G. Tulasiram Das, "Simulation of Real and Reactive Power Flow Control With UPFC Connected to A Transmission Line". Journal of Theoretical and Applied Information Technology, 2008.

[57] Samina Elyas Mubeen, R. K. Nema, and Gayatri Agnihotri, "Power Flow Control With UPFC in Power Transmission System". Engineering and Technology Volume 30 July 2008 ISSN 1307-6884

[58] K. Krishnaveni, and G. Tulasi Ram Das, "Ann Based Control Patterns Estimator for UPFC Used in Power Flow Problem". Journal of Theoretical and Applied Information Technology, 2007.

[59] S. Tara Kalyani, and G. Tulasiram Das, "Simulation of D-Q Control System For A Unified Power Flow Controller ". ARPN Journal of Engineering and Applied Sciences, vol. 2, no. 6, December 2007.

[60] M. A. Abido, "Power System Stability Enhancement Using FACTS Controllers: A Review". The Arabian Journal for Science and Engineering, Voulem 34, Number 2B, April 2009.

[61] Ali T. Al-Awami, A.A. Abido, and Y. L. Abdel-Magid, “A Comparative Study on Effectiveness of Robust FACTS Stabilizers for Power System Stability Enhancement”. The Arabian Journal for Science and Engineering, Voulem 33, Number 2B, October 2008.

[62] Mahyar Zarghami, and Mariesa L. Crow, “Discussion on Effective Control of Inter-Area Oscillation by UPFCs”. IEEE transactions on power systems, October 2007.

VITA

Name: MOHAMMED ABDUL-RAOUF M. AL-GHAZWI

Education: *Master of Science (M.S.)* degree in Electrical Engineering

King Fahd University of Petroleum & Minerals

Bachelor of Engineering (B.E.) degree in Electrical Engineering

King Fahd University of Petroleum & Minerals

Date of Birth: 19th July 1981

Place of Birth: Al-Qateef, Saudi Arabia

Contact: mohgh99@yahoo.com